AUTOMATIC PARTICLE COUNTING USING AN ACOUSTIC TRANSDUCER

by

GEORGE FARID HADDAD
B.S. Cleveland State University, 1989

A thesis submitted in partial fulfillment of the requirements
for the degree of Master of Science
in the Department of Mechanical, Materials and Aerospace Engineering
in the College of Engineering and Computer Science
at the University of Central Florida
Orlando, Florida

Spring Term
2005

ABSTRACT

Aerosol particle detection and determination finds important applications in the commercial, military and aerospace sectors. Monitoring of clean room environments, and spacecraft integration and check out facilities are some of the most important applications. In the early days test filters were examined with a microscope to determine the number and size of particles that were being removed from air. Today, most of the commercially available clean room airborne particle counters work on a light scattering principle. They are referred to as Optical Particle Counter or OPC. Essentially, they utilize a very bright laser light source to illuminate the particles. The burst of light energy is converted into a pulse of electrical energy. By measuring the height of the signal and counting the number of pulses the sizes and quantities of particles could thus be determined. The microscope and the OPC techniques have their limitations. The microscope technique is a post contamination assessment technique and the OPC is costly, hard to maintain, lack in counting efficiency and is not mobile. This experimental study demonstrates a novel and inexpensive particle detection technique which is based on the acoustic signature of airborne particles as they are accelerated through an acoustic transducer. The transducer consists of an inlet converging nozzle, a capillary tube and an expansion section. If the air is laden with particles, as the flow accelerates through the inlet, the particles cannot follow the large change in velocity due to their inertia. Vortices

are generated as air flows over the particles prior to entering the capillary. These vortices are believed to generate sound, which is amplified by the transducer acting as an organ pipe. This sound emission if measured contains frequencies that are harmonics of the natural frequency of the transducer's air column.

Results show how the frequency content of the acoustic signature relates to the fundamental frequency of the transducer's air column. The transducer is able to detect micron sized particles (5 to 50 micron) and the sound intensity is a function of the flowrate but not of particle size. This study also shows the ability of the transducer to determine particle concentration as low as few parts per liter (ppl) and compare the data with that obtained from a commercially available aerodynamic particle sizer.

ACKNOWLEDGMENTS

This experimental study was supported by NASA Kennedy Space Center (KSC) under NASA grant NAG10-0319. The author wishes to sincerely thank the Launch Service Provider (LSP) managements at KSC especially my immediate supervisor Ms. Denise Pham for her support to my Master Degree Course work and her support to this study. Also special thanks to Mr. Pat Hanan, Mr. Darren Bedell, and Mr. James Robinson for their support and for providing the opportunity to advance this new concept in particle detection.

Special thanks to my advisor Dr. Ruey-Hung Chen whose dedication to this idea and this work was a great inspiration to me. Dr. Chen was the initiator of the early phase of this work. A special acknowledgment to Dr. Marcos Chaos who was very instrumental in the design, fabrication and testing of the acoustic transducer. Finally I would like to thank my wife Wendy and my sons Matthew, Andrew and Peter for their patience with me and their support to my Master Degree Studies at UCF.

TABLE OF CONTENTS

LIST OF FIGURES

LIST OF TABLES

CHAPTER ONE: INTRODUCTION

Detection of small particles in the micron range and at low concentration continues to be a challenge for many industries and in many applications especially for the aerospace and electronic industries. The current particle counters are expensive, as they don't count particles directly but instead count flashes of light scattered by particles. They are bulky and require a knowledgeable user as they employ lasers and optics. This thesis investigates the capabilities of detecting and counting small particles with an acoustic transducer. The acoustic transducer proposed here is lightweight, has low cost and good mobility and counts particle directly based on the acoustic radiation from the particles. The transducer shown in Figure 2.1, Chapter two uses a glass tube consisting of an inlet section, a contraction, a capillary section, and an outlet section with an expansion. Air laden particles are drawn into the capillary section by a pump.

In the 1950s to 1960s Langer [1] observed that dust particles, when introduced into an air stream, produce a noticeable change in the flow noise. Langer noticed this observation in a vacuum cleaner hose that was used to collect dust particles from an aerosol generator. He concluded that the noise was created at the point where the hose was constricted by a clamp. Thus the particle size is correlated with the noise generated when the particles are drawn with air through a flow contraction. Langer's work on the particle counter proceeded in an empirical manner in the absence of a working theory

explaining the performance of the acoustic sensor. Langer optimized the design of his acoustic particle counter which is capable of detecting particles down to 5 microns in diameter. He also reported that the noise signal was probably generated near or just inside the exit cavity, and that there is no pronounced change in signal amplitude with variation of particle size. Langer [1-2] hypothesized that a low- pressure shock wave is behind the generation of the noise pulse. A large difference in velocity suddenly develops between the air and the aerosol particles, and the energy excess of the particles is dissipated in the form of this low-pressure shock wave.

Karuhn [3] also used a capillary to draw particle laden air and claimed to detect the oscillating shock wave at the exit of the capillary. He hypothesized that particles initiate a toroidal turbulence in the capillary tube which is proportional to the particle sizes. The toroids cause a change in the flow velocity and interact with a stationary shock front established by the laminar jet. This interaction results in oscillations of the shock front thereby producing sound. Mills and Chen [4] reported that for a shock wave to occur in the diverging section of the capillary the flow must be supersonic. Supersonic flows will occur in the diverging section of the capillary for pressure ratios downstream to upstream less than 0.528 for air [5]. In reference [1] a pressure drop of 18 cm Hg was reported across the capillary. Such a pressure drop was not sufficient to cause the capillary to produce supersonic flow. Therefore, there should be no supersonic expansion, and shock wave does not appear at the capillary exit. Also detection of acoustic signals both upstream and downstream of the capillary further rules out shock wave phenomenon as the source of signals generated in the acoustic transducer. Chen et al [6] determined

that acoustic signals were generated as particles were accelerated through the transducer's contraction. Owing to their inertia, suspended particles cannot follow the rapidly accelerating flowfield. A turbulent wake is thus generated as air rushes behind the particles, which disturbs the air column within the inlet and capillary sections of the transducer thereby generating noise.

The objective of the present work is to gain a better understanding into the processes taking place in the acoustic transducer. The particle motion through the contraction and capillary sections of the transducer tube is investigated. The motion of particles with sizes of 2, 5, 15, and 59 micron were simulated assuming a system flowrate of 45 L/min. The results of such a simulation are represented in details in Chapter Three – particle motion. The particle detection ability of the transducer as a function of particle size and system flowrate is determined. Polysterene Latex (PSL) spherical particles with sizes of 5, 15 and 50 micron particles were introduced into the test chamber and their acoustic signal time trace and frequency content were evaluated for 40 L/min and 50 L/min. The acoustic signal strength was also measured for PSL particles of 5, 15 and 50 micron for different flowrates. Finally the capability of the transducer for concentration measurement was tested, and a correlation was sought between the concentration measured by the acoustic transducer and that measured by a commercially available aerodynamic sizer [7].

CHAPTER TWO: EXPERIMENTAL SET UP

This chapter provides detailed information concerning the design and construction of the acoustic transducer experimental setup. The physical properties of the acoustic transducer will be described first followed by the housing chambers and instrumentation, and the electronic hardware and software used for data acquisition.

Acoustic Transducer

As shown in Figure 2.1, the acoustic transducer is a tube of variable cross section, consisting of an inlet section, a contraction and a capillary section followed by the outlet portion of the tube. The overall length of the tube is 148.7 mm. The inlet and outlet diameters are 10 mm and 12.5 mm respectively. The transducer is made of borosilicate glass which assures a smooth internal surface; any roughness would trip the boundary layer and could lead to early development of turbulence interfering with any acoustic signals generated. Manufacturing of the transducer was accomplished via scientific glass blowing (Glassform Glassblowing Co., MI). Dimension accuracy provided by this method is usually in the order of 0.1 mm approximately.

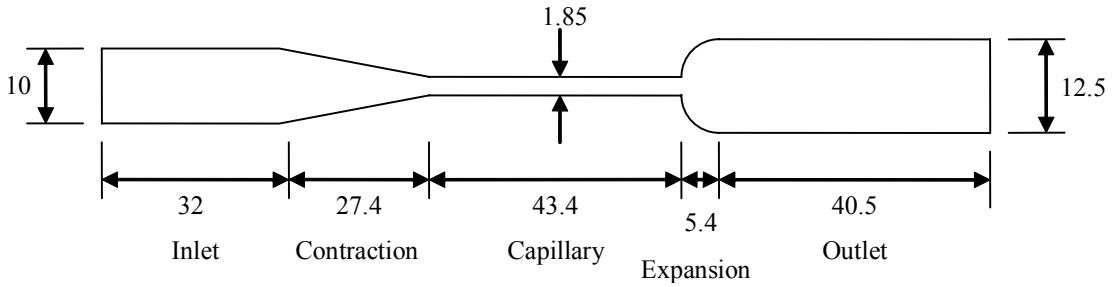

Figure 2.1: The acoustic transducer (all dimensions in mm).

Acrylic Chambers and Instrumentation

Figure 2.2 presents a schematic of the experimental set up of the acoustic transducer. All commercially available parts used in the setup are listed in Table 1. The acoustic transducer was placed across two separate but adjoining chambers made of acrylic plastic. The chambers had volumes of 23 L and 4.7 L corresponding to the inlet side and outlet sections of the transducer respectively. The larger inlet chamber contained all instrumentation, and was open to room air through a quartz microfiber filter. The outlet chamber was connected to a vacuum pump through a rotameter used to control and measure the flowrate. Both chambers contained bolt-on lids for easy instrumentation access, and are bolted onto a central flange that supported the acoustic transducer. Detailed drawings of the chambers can be found in Appendix A.

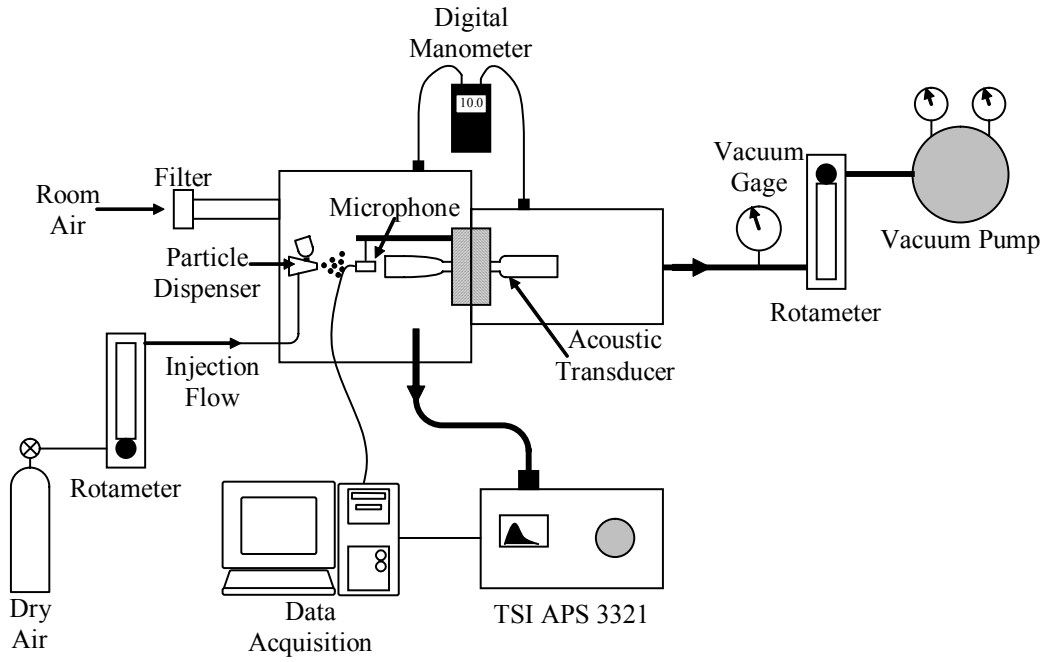

Figure 2.2: Experimental setup.

Table 2.1: Parts list.

Item	Vendor	Model/Part Number
Filter	Whatman	EPM2000/1882047
Manometer	Dwyer Instruments and Control	Series 475 Mark III
Microphone	Knowles Electronics, Inc.	BL-1994
Particle injector	Paasche Airbrush Company	AEC Air Eraser
Rotameter (injection)	Aalborg Instruments and Control, Inc.	044-40G
Rotameter (vacuum)	Aalborg Instruments and Control, Inc.	044-40C
Vacuum gage	Omega Engineering, Inc.	DPG1000B-30V100G
Vacuum pump	GAST Manufacturing Corp.	0523-V4-SG588DX

Since the system was operated under vacuum, effort was placed in properly sealing the chambers. After manufacturing the chambers, acrylic shavings (left over from the manufacturing process) were mixed with a solvent agent (TAP Plastics, CA) which produced a glue-like substance. This liquid acrylic mix was used to coat all seams in the

chambers. On account of the capillary action of the solvent, all gaps and crevices in the chambers were filled. As explained above, the chambers bolted onto the central flange and consisted of lids that also bolted onto the chambers. The joints between the chambers and the flange were sealed by tailor-made gaskets cut from 40A Durometer latex rubber sheets 1.25 mm thick. The sealed chambers are shown in the actual image found in Figure 2.3. As seen in Figures 2.3 and 2.4 the acoustic transducer was supported by two aluminum blocks which squeezed the central flange between them. Bolts were used to hold the supports in place. Silicone o-rings were seated into the blocks to provide an air-tight seal. The chamber assembly was pressure tested for leaks using a liquid leak detector on all seams and joints.

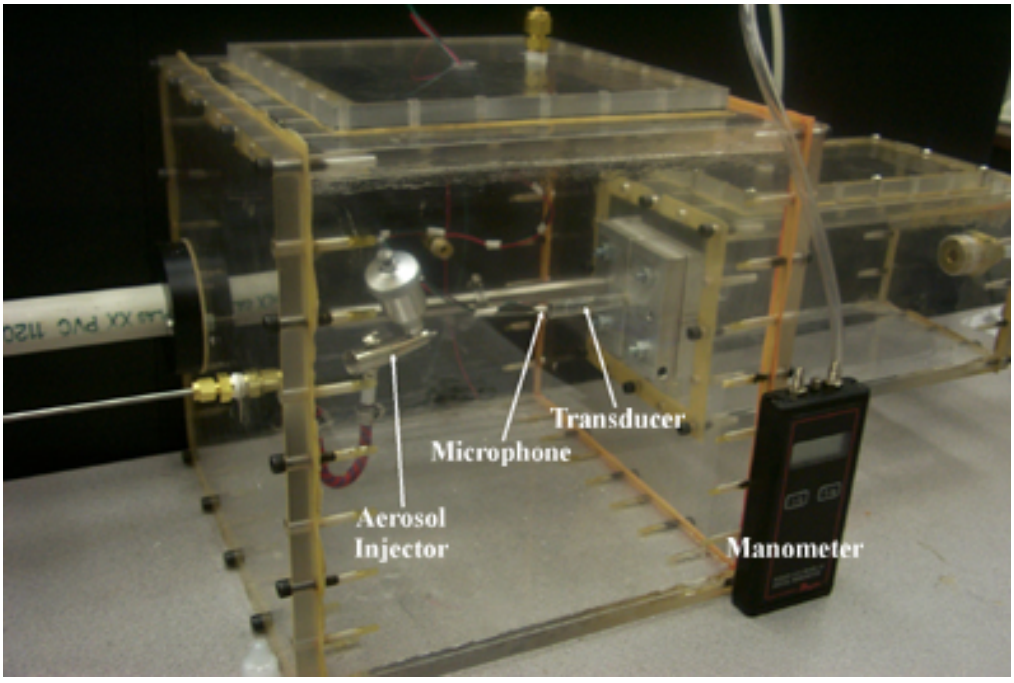

Figure 2.3: Acrylic chambers.

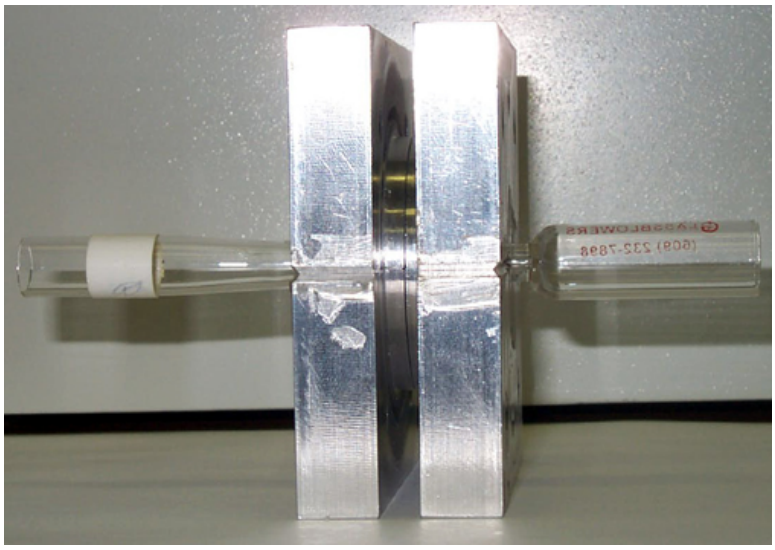

Figure 2.4: Acoustic transducer central flange support.

PSL aerosol particles with known nominal sizes (Duke Sientific Corp., CA) were injected into the inlet chamber using an air eraser tool. The particles were dispersed by moisture free pressurized bottled air passing through a rotameter in order to control the amount of particles injected. The acoustic signals generated as particle laden air accelerated through the transducer were measured by a small (6 x 4 x 2 mm approximately) electret condenser microphone used in hearing aid applications. This microphone has a high sensitivity and exhibits a flat broadband response over a wide frequency range (0 – 10000 Hz) as shown in Figure 2.5. The microphone was placed along the central axis of the acoustic transducer 5 mm from the inlet which provided signals with the best signal-to-noise ratio (SNR). The microphone was supported by a steel rod which threaded into the aluminum flange holding the acoustic transducer (see

Figure 2.3). The microphone was wired using a source follower arrangement as pictured in Figure 2.6. By wiring the microphone this way, the overall broadband sensitivity and maximum sound pressure level that can be detected by the microphone can be improved. A 3 V battery powered the microphone; typical output signal traces had peak-to-peak amplitudes ranging from 0 - 1 V.

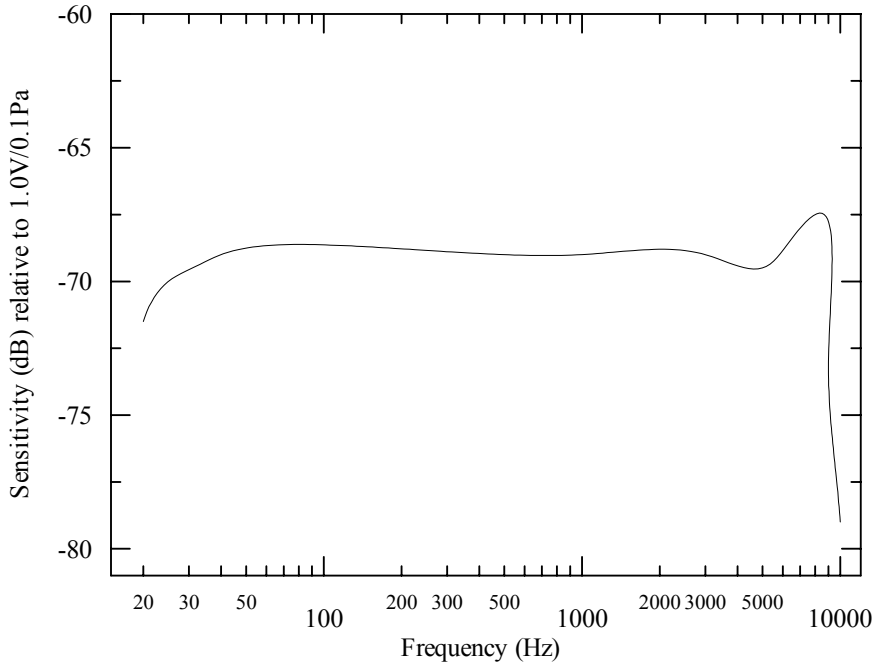

Figure 2.5: Microphone sensitivity response.

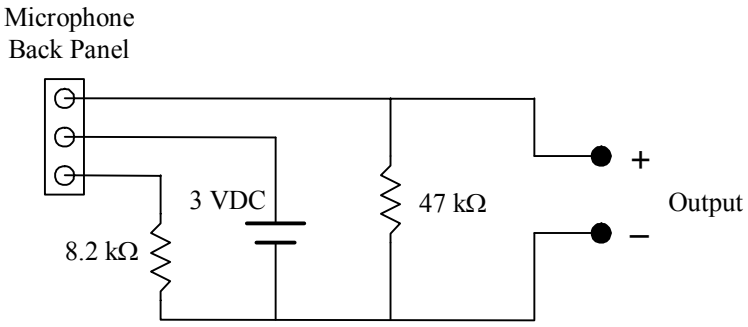

Figure 2.6: Microphone source follower wiring diagram.

A laboratory vacuum pump drew room air through the system. The pump was connected to the outlet side of the chamber via polyethylene tubing (½" OD) part of which was lined with steel wire in order to prevent its collapse under vacuum. The pump inlet was fitted with appropriate filters to prevent any particles from damaging the pump's vanes. Flowrate through the system was monitored redundantly by measuring the pressure drop across the inlet and outlet chambers (i.e. across the acoustic transducer) ,and also by a rotameter placed upstream of the vacuum pump. A calibration curve was obtained to correlate the pressure ratio between outlet and inlet chambers with flowrate measured by the rotameter and is shown in Figure 2.7. As is to be expected, the flowrate is seen to be proportional to the square root of the chamber pressure drop. This relationship may prove useful if the rotameter were to be removed from the setup in future applications in order to minimize system pressure losses. For all the experiments reported herein, the rotameter was used to determine the system flowrate.

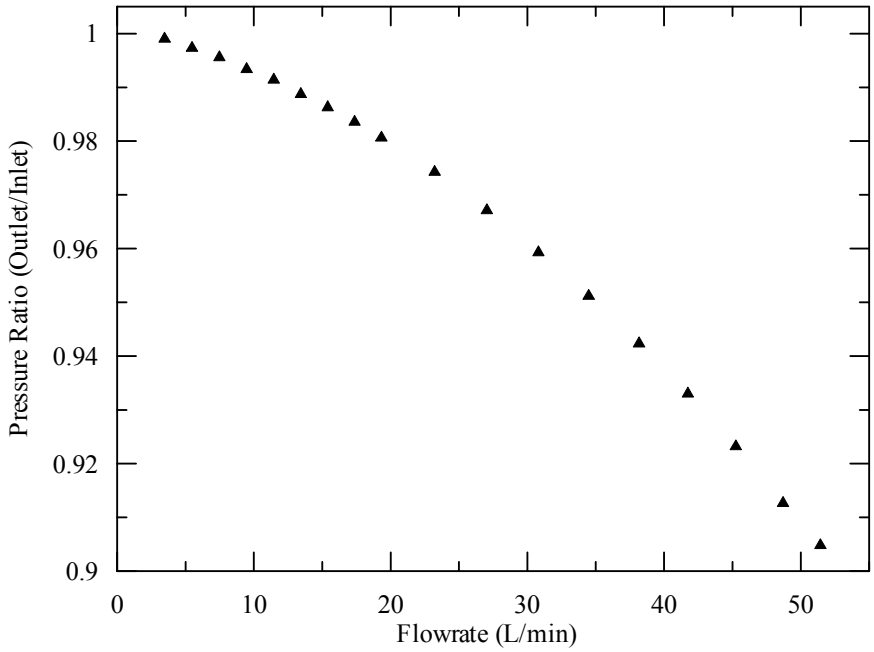

Figure 2.7: Flowrate vs. chamber pressure drop.

Since the system was operated under vacuum, the rotameter had to be modified in order to obtain accurate flow readings by moving the control valve from the inlet to the outlet section of the meter. The rotameter is factory calibrated under standard pressure and temperature. Therefore its indicated flowrate under vacuum does not represent the actual flowrate. The correction is expressed by Equation 1 below:

$$Q_A = Q_I \sqrt{\frac{P_A}{P_{CAL}} \frac{T_{CAL}}{T_A}} \qquad (1)$$

Where Q_A and Q_I are the actual and indicated flowrates, respectively, P_A and T_A are the corresponding actual pressure and temperature respectively and P_{CAL} and T_{CAL} are respectively the pressure and temperature, at which the rotameter was calibrated. Both T_A and T_{CAL} can be considered equal since all experiments were performed at room (i.e. standard) temperature. Hence, the actual flowrate through the system is determined by the vacuum pressure (since P_{CAL} = 1 atm) which was measured by a digital vacuum gage.

It is to be noted that the maximum flowrate that could be attained with the setup described above was on the order of 50 L/min approximately. Thus it is assured that the acoustic transducer will not operate under choked (i.e. sonic) conditions. Assuming the speed of sound under standard conditions to be nearly 350 m/s, the flowrate through the capillary section of the acoustic transducer (1.85 mm ID see Figure 2.1) under sonic flow conditions would be 60 L/min, approximately. . Furthermore, the data in Figure 2.7 indicates that the pressure ratio between the outlet and inlet chambers is always above 0.9 for the range of flowrates tested in this study. For sonic conditions, this ratio would have to be at least 0.528 [7]. The flow through the transducer, however, can reach high velocities, and air compressibility effects are to be expected

As shown in Figure 2.2, an aerodynamic particle sizer (TSI Model APS 3321) was connected to the inlet chamber. This instrument continuously monitored the concentration of particles in the size range between 0.5 μm and 20 μm by drawing a constant flowrate of 5 L/min from the inlet chamber. The APS was connected to a data acquisition computer (see section below) which also collected the microphone signal.

Thus, simultaneous concentration measurements could be taken by both the APS and the transducer, which would provide a correlation between the two instruments.

Data Acquisition

Microphone output voltage signals (Figure 2.6) were gathered and analyzed using a computer controlled data acquisition system. The electrical signal from the microphone was transmitted to an external connector block (National Instruments CB-68LP), attached to a computer-based data acquisition board (National Instruments PCI-6034E). The data acquisition board was controlled by LabView, a software package from National Instruments. LabView is a graphical user interface that can be used to create "virtual" instruments to gather, analyze and display data. Two such graphical programs were created, and the diagrams can be found in Appendix B.

The first program gathers data at a user specified rate (from 0 to 20 kHz) and stops the acquisition after certain number of points are collected (also user specified). The data is conveniently saved in a text file in column format, which can be easily read by any spreadsheet application. The user also has the option of controlling the accuracy (i.e. significant digits) of the gathered voltage data. Furthermore, the signal acquired by this program is plotted, real time, on the computer monitor. This program was used to obtain raw data from the microphone to be further analyzed by spreadsheet programs such as Microsoft Excel.

The second program was developed for real time display of the Fourier transform of the microphone signal. This program continuously monitors the signal from the microphone displaying it, in a chart format, on the computer screen. A user-specified number of data points (which must be a power of 2) are sent to a buffer for Fourier analysis. The result of this analysis (i.e. frequency components of the signal) is also displayed graphically on the computer screen. This program was useful in determining frequency content of the microphone signal.

CHAPTER THREE: ANALYSIS OF PARTICLE MOTION

Chapter three analyzes the particle motion through the transducer. The governing equations for particle motion are discussed and the numerical solutions are presented.

Governing Equations of Particle Motion

As discussed by Chen *et al*. [6], the audible noise generated as particles flow through the acoustic transducer is attributed to the inability of the particles to follow perfectly the accelerating airflow around them as they enter the transducer contraction. This leads to flow separation around the particles followed by a vortex wake which causes a pressure disturbance amplified by the inlet section of the transducer (acting as an organ pipe), thus generating noise. In fact, during the experiments described herein, the inlet chamber was open and wires of different sizes were introduced in the inlet section of the transducer. These wires had a blunt (i.e. spherical) tip. As the wire tip neared the capillary, acoustic signals were picked up by the microphone. This lends further support to the fact that vortices produced in the wake flow are responsible for the acoustic radiation. Placing the wire almost at the entrance of the capillary produced a continuous tone; at this location the flow speed is high, and the vortices emanating from the wire tip are shed at a high frequency generating an almost continuous signal.

It is of interest, thus, to determine if the particle velocity lag is sufficient enough for the flow to separate around the spherical PSL particles tested. This was addressed by investigating the particle motion through the contraction and capillary sections of the transducer tube. As the particles enter the contraction carried by the air flow, they are accelerated by the drag force generated as air flow past the particles. The forces governing the particle motion along the transducer axial direction is shown in Figure 3.1. Motion of the particle in the transverse direction is not considered as body forces due to gravity are negligible when compared to the drag forces the particles experience in the contraction.

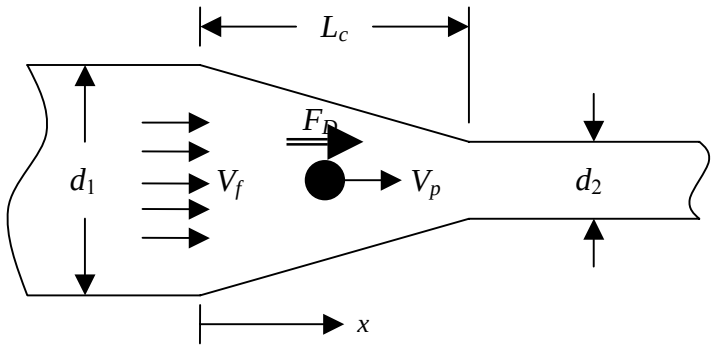

Figure 3.1: Diagram of particle motion through the transducer

A force balance in the *x* direction (Figure 3.1) leads to the following equation:

$$F_D = ma_p = m\frac{dV_p}{dt}\,;\; m = \rho_p V_p$$

$$\frac{dV_p}{dt} = \frac{F_D}{\rho_p \forall_p} \tag{1}$$

where a_p is the particle acceleration, F_D the drag force, m the particle mass, V_p the particle velocity, ρ_p the particle density, and $\forall_p$ is the particle volume. The drag force F_D is a nonlinear function of both the particle velocity and the velocity of the surrounding airflow, V_f:

$$F_D = \frac{1}{2}\rho_f C_D A_p \left(V_f - V_p\right)^2 \tag{2}$$

Where ρ_f is the air density, C_D is the drag coefficient, and A_p is the particle cross-sectional area. The added mass term (see, for example, Auton *et al* [8]), classically found in mechanics, due to the resistance of the surrounding fluid to acceleration has been neglected as the fluid density is much lower than the particle density.

Introducing geometric expressions for the particle (sphere) area and volume and combining Equations (1) and (2), the particle acceleration is then:

$$\frac{dV_p}{dt} = \frac{3}{4}\frac{\rho_f}{\rho_p} C_D \frac{\left(V_f - V_p\right)^2}{d_p} \tag{3}$$

where d_p is the particle diameter. Equation (3) combined with Equation (4):

$$\frac{dx_p}{dt} = V_p \tag{4}$$

where x_p is the particle position, present a system of two first-order differential equations solving for the particle velocity and position within the transducer tube.

The quantities C_D and V_f terms in Equation (3) need to be explained further as their accurate evaluation is necessary in order to solve the differential equations. V_f is constant before and after the contraction but changes as a function of the tube diameter as air flows through the contraction. The tube tapers linearly from a diameter d_1 at the contraction inlet to a diameter d_2 at the entrance to the capillary over the distance L_c (see Figure 3.1). If the volumetric flow through the system is Q then the air velocity through the contraction varies as follows:

$$V_f = \frac{4Q}{\pi}\left[d_1 - \left(\frac{d_1 - d_2}{L_c} \right) x \right]^{-2} \tag{5}$$

The sphere drag coefficient, C_D, is a function of the Reynolds number based on the velocity slip experienced by the particle ($V_f - V_p$). The particle Reynolds number is given as:

$$Re = \frac{\rho_f (V_f - V_p) d_p}{\mu_f} \tag{6}$$

where μ_f is the air viscosity. It is expected that, initially, the particle Reynolds number in the initial stage of flow acceleration is very low (Re < 0.5) and Stokes' drag relations are applicable (Stokes [9]); *Re* increases as the particle moves further into the contraction owing to increased relativevelocity. Once the Reynolds number increases beyond 0.5, the expressions of Oseen [10] and Clift *et al*. [11] are applicable. A summary of the expressions for the drag coefficient for different Re range is presented below:

$$C_D = \frac{24}{Re}\ ;\ Re < 0.5 \text{ (Stokes [9])} \tag{7}$$

$$C_D = \frac{24}{Re}\left(1+\frac{3}{16}Re\right);\ 0.5 < Re < 1 \text{ (Oseen [10])} \tag{8}$$

$$C_D = \frac{24}{Re}\left(1+0.15\,Re^{0.687}\right);\ 1 < Re < 1000 \text{ (Clift } et\ al. \text{ [11])} \tag{9}$$

$$C_D = 0.44\ ;\ 1000 < Re < 3\text{x}10^5 \text{ (White [12])} \tag{10}$$

For high system flowrates, air compressibility effects need to be taken into account since air velocities can reach near sonic speeds as the flow approaches the capillary. This changes the air density, ρ_f, considerably which is needed to calculate Reynolds number (Equation 6) and particle acceleration (Equation 3). For simplicity, the air viscosity, μ_f, which depends primarily on temperature, is assumed constant. The change in air density is given as follows (John, [13]):

$$\rho_f = \rho_0\left(1+\frac{\gamma-1}{2}M^2\right)^{-1/\gamma-1} \tag{11}$$

where ρ_0 is the air density at standard conditions (20°C and 1 atm, ρ_0 = 1.2041 kg/m^3), γ the specific heat ratio (1.4 for air), and M the Mach number of the flow defined as:

$$M = \frac{V_f}{\sqrt{\gamma RT}} \tag{12}$$

where R = 287 J/kg K is the air gas constant and T is the temperature (taken to be equal to 20°C or 293.15 K).

$$\text{Let } \frac{dV_p}{dt} = f_1\left(x_p, V_p\right); \quad \frac{dx_p}{dt} = f_2\left(V_p\right)$$

$$\begin{cases} \Delta v_1 = h f_1\left(x_{p_n}, V_{p_n}\right) \\ \Delta x_1 = h f_2\left(V_{p_n}\right) \end{cases}$$

$$\begin{cases} \Delta v_2 = h f_1\left(x_{p_n} + \frac{\Delta x_1}{2}, V_{p_n} + \frac{\Delta v_1}{2}\right) \\ \Delta x_2 = h f_2\left(V_{p_n} + \frac{\Delta v_1}{2}\right) \end{cases}$$

$$\begin{cases} \Delta v_3 = h f_1\left(x_{p_n} + \frac{\Delta x_2}{2}, V_{p_n} + \frac{\Delta v_2}{2}\right) \\ \Delta x_3 = h f_2\left(V_{p_n} + \frac{\Delta v_2}{2}\right) \end{cases}$$

$$\begin{cases} \Delta v_4 = h f_1\left(x_{p_n} + \Delta x_3, V_{p_n} + \Delta v_3\right) \\ \Delta x_4 = h f_2\left(V_{p_n} + \Delta v_3\right) \end{cases}$$

$$\left.\begin{aligned} V_{p_{n+1}} &= V_{p_n} + \frac{1}{6}\left(\Delta v_1 + 2\Delta v_2 + 2\Delta v_3 + \Delta v_4\right) \\ x_{p_{n+1}} &= x_{p_n} + \frac{1}{6}\left(\Delta x_1 + 2\Delta x_2 + 2\Delta x_3 + \Delta x_4\right) \end{aligned}\right\} \text{for } n = 0,1,2,\ldots$$

Figure 3.2: Runge-Kutta scheme

Numerical Solution: Governing Differential Equations

With the help of these equations, the system of differential equations formed by Equations (3) and (4) can now be solved. Since these equations are nonlinear, a numerical approach is employed in order to solve the system. The classical fourth-order Runge-Kutta algorithm (Akai [14]) was used. The classical Runge-Kutta algorithm starts from given boundary conditions (i.e. particle position and velocity as the particle enters

the contraction) and marches the solution to a new position and particle velocity using a fixed time step *h*. The velocity and position updates come from a weighted average of the derivatives in Equations (3) and (4). As can be inferred from these equations, Equation (3) is a function of particle position as well as particle velocity whereas Equation (4) is solely a function of particle velocity. With this in mind the numerical scheme can be constructed as shown in Figure 3.2.

The algorithm starts with known values at the entrance to the contraction section of the transducer tube, namely x_{p_0} and V_{p_0}. As shown in Figure 3.2, the algorithm evaluates Equations (3) and (4) at intermediate velocities and positions yielding updated values for the next particle position and velocity (i.e. $x_{p_{n+1}}$ and $V_{p_{n+1}}$). At each position, Equations (5), (12), (11), (6), and (7) through (10), in this order, need to be evaluated to provide inputs for Equations (3) and (4). The scheme in Figure 3.2 is iteratively performed until the particle position (i.e. x_p) has reached the end of the capillary. The time step size *h* chosen needs to be sufficiently small, as the error introduced by the numerical approach depends on this value. For the current application *h* was chosen to be a fraction of the time it takes the airflow to move through the contraction which can be found by integrating Equation (5) from 0 to L_c leading to the following expression:

$$t_c = \frac{\pi L_c}{Q}\left(d_1^2 + d_1 d_2 + d_2^2\right) \tag{13}$$

Numerical Solution : FORTRAN Program

Based on the above numerical scheme, a FORTRAN program was developed to solve for the particle motion as it travels through the transducer. The source code for this program can be found in the Appendix C. The program was executed using the geometrical parameters of the transducer described in this report. Different particles sizes were considered in an effort to determine how particle size affects the motion of suspended particles as they are accelerated in the transducer tube. A time step of $h = t_c/100$ was chosen. Since the experiments described herein used PSL spheres, the particle density was set at $\rho_p = 1.05$ g/cm^3 a value supplied by the manufacturer of the spheres (Duke Scientific Corp.). The motion of particles with sizes of 2, 5, 15, and 50 μm were simulated assuming a system flowrate of 45 L/min and the results are summarized in Figure 4.1. It can be clearly seen how size has a drastic effect in the velocity the particles acquire in the contraction and capillary sections of the transducer. Except for the 2 μm particles, which closely follows the flow speed reaching approximately 80% of the gas flow velocity at the entrance to the capillary, all other particles never reach the flow velocity at any point within the transducer. This difference between flow and particle velocities for $d_p > 2$ μm may give rise to flow shedding behind the particles leading to pressure disturbances in the flow.

CHAPTER FOUR: RESULTS AND DISCUSSION

Chapter four evaluates the acoustic signals generated by the transducer, the acoustic signal strength, and the concentration capabilities of the transducer.

Particle Size

An inspection of Figure 4.1 suggests that except for the 2 micron particles, the maximum velocity lag is reached only at the end of the contraction. Table 2 lists the velocity lag (i.e. $V_f - V_p$) and the Reynolds number based on the particle diameter for the different particle sizes at the end of the contraction. For the 2 μm particle at the point of maximum acceleration and velocity slip, the Reynolds number approaches that of a creeping flow. As the particle size increases such as the Reynolds number is about 40, the wake behind a sphere becomes unstable. At a Reynolds number of about 100 (i.e. the 15 μm particle) continuous toroidal vortices are present in the sphere wake. For $Re > 400$ the vortices are no longer continuous and are periodically shed from the spherical particles (Achenbach, [15]). Thus, for particles larger than 2 μm, unsteady wakes and vortices are shed from the particles as they are accelerated through the acoustic transducer. These unsteady phenomena cause pressure disturbances which excite the air column inside the transducer generating the acoustic signals shown in previous sections.

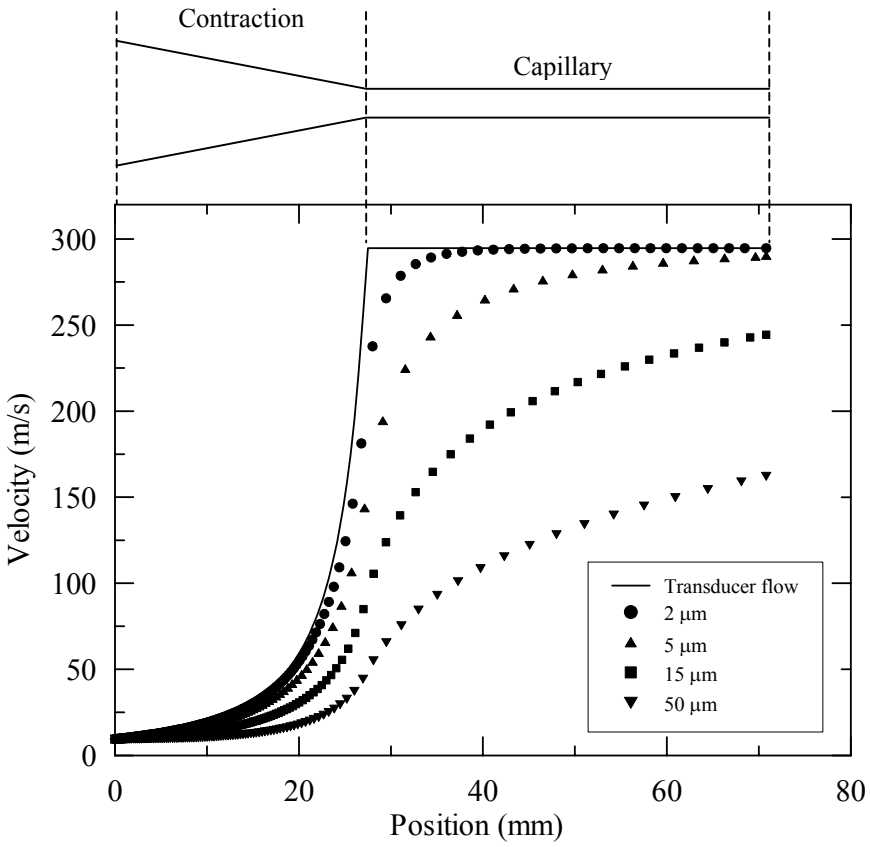

Figure 4.1: Effect of particle size on particle velocity.

Table 4.1: Velocity and Reynolds number at the entrance to the capillary

Particle Size (μm)	$V_f - V_p$ *(m/s)*	Re
2	62.1	8
5	128.3	33
15	204.5	142
50	247.1	574

Acoustic Signals

When particles were present in the inlet chamber, audible click-type noise signals were generated by the transducer for flowrates above 30 L/min. At such flowrates, Reynolds numbers based on the diameter of the particles in both the inlet and capillary sections are well above the critical value of 2,100 for turbulent pipe flow [12]. The flow in the transducer, however, has been shown to be laminar [1, 3] since the walls are smooth and the air residence time is short both of which delay the development of turbulence. Figure 4.2 shows a typical acoustic signal for 50 micron PSL particles with flow rates of 40 L/min and 50 L/min. Figure 4.3 shows the corresponding acoustic signal for a 15 micron particle, and Figure 4.4 for a 5 micron PSL particle. It is seen that the acoustic signals for the different particle sizes and flowrates are qualitatively similar. The trace for all particles starts with a negative voltage, indicating a drop in pressure, followed by a high frequency signal which decays within 3 ms to 10 ms. This leading pressure drop is expected as previous studies [4] shown. It was also shown [4] that signals collected downstream of the transducer outlet begin as a compression wave (i.e. a pressure rise). The maximum signal-to-noise ratio that could be achieved with the current transducer was on the order of 20/1 for flowrates near 50 L/min, and 2/1 for the lowest flowrate (50 L/min). It has previously been reported [1] that signal strength can be increased by shortening the capillary tube or increasing the capillary diameter.

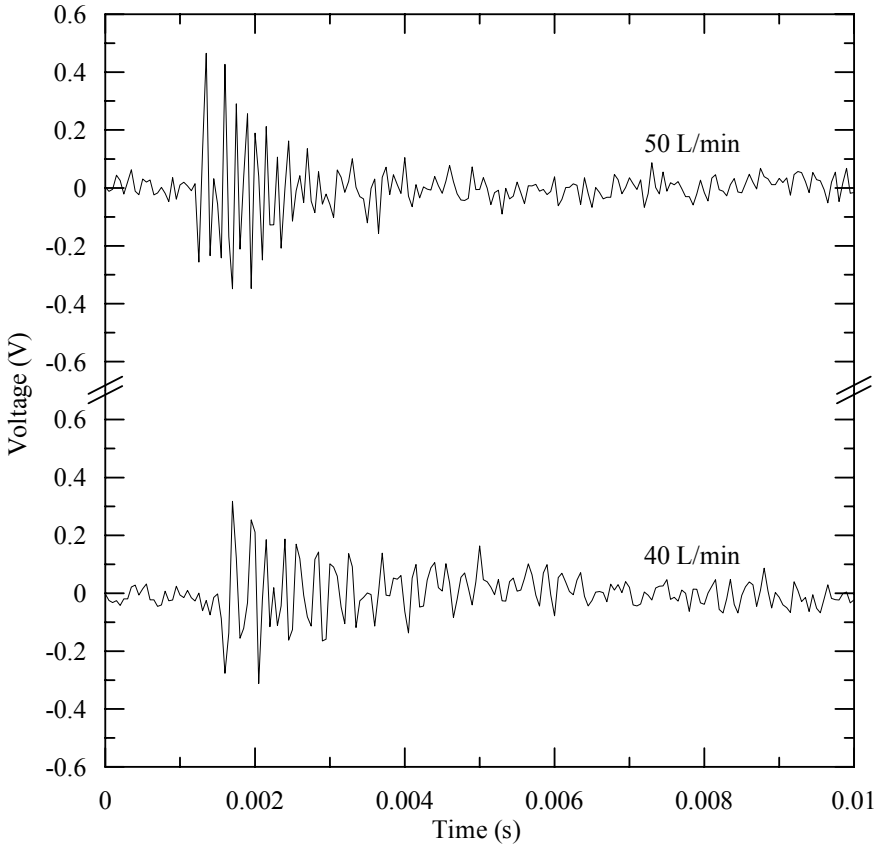

Figure 4.2: Single particle acoustic signal time trace for 50 μm PSL particles.

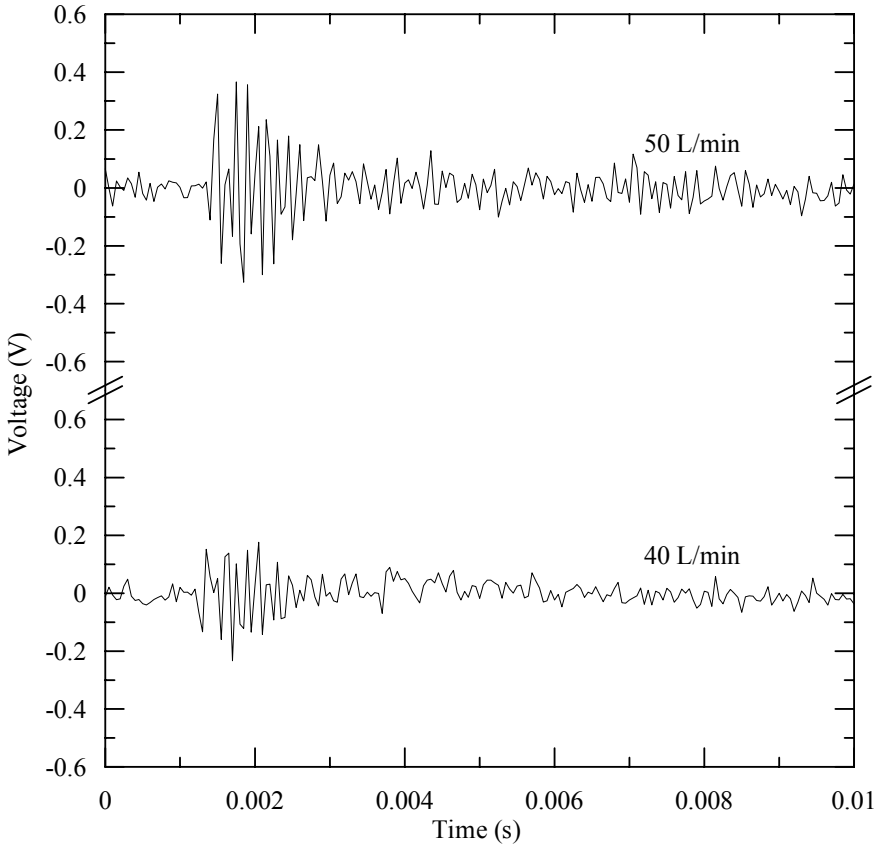

Figure 4.3: Single particle acoustic signal time trace for 15 μm PSL particles.

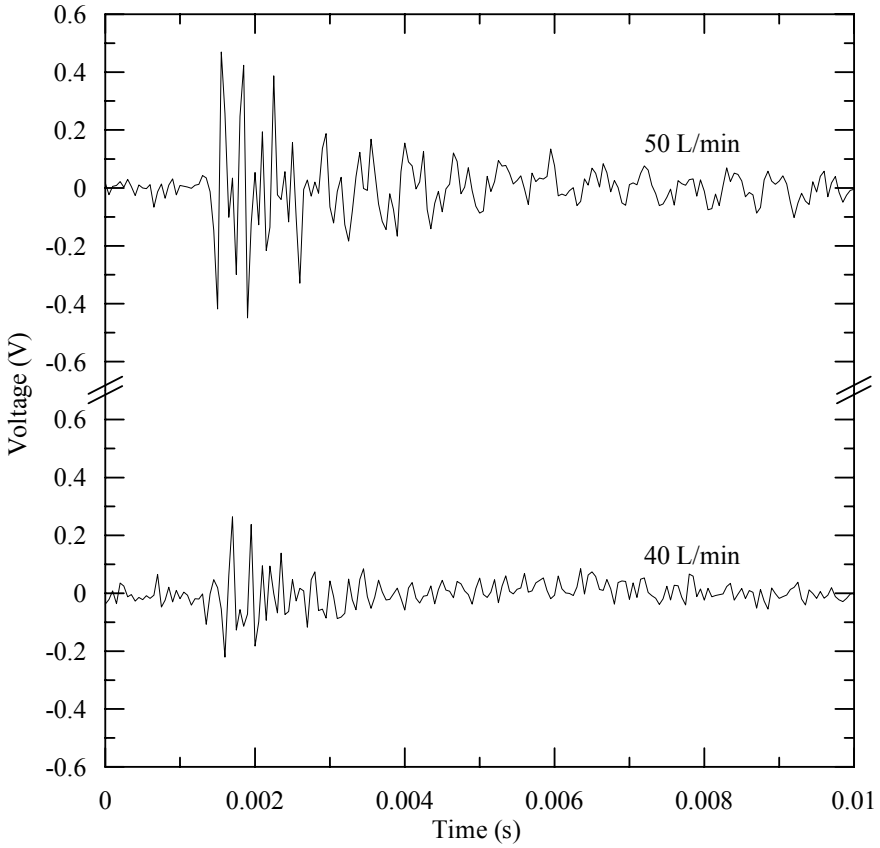

Figure 4.4: Single particle acoustic signal time trace for 5 μm PSL particles.

A Fourier analysis of the acoustic signals was done in Excel using the Data analysis package to look at the Power spectrum of the signals. The data acquisition board gathered samples at a maximum rate of 20,000 samples per seconds, so only frequencies up to 10,000 Hz can be discerned (i.e. Nyquist criterion). Noise was present in the system due to ground loop electrical coupling and the sound generated by the pump (although this sound is very faint inside the closed inlet chamber). The frequency components of this noise were removed by subtracting microphone samples taken when

no particles were present in the system. The FFT noise analysis is shown in Figure 4.5. Note that the 60, 120, 180, 240 Hz noise components are due to ground loop electrical noise, and the higher frequency components are probably introduced by the amplification circuit of the data acquisition board.

The spectral content of the signal of Figure 4.2 is shown in Figure 4.6. Three distinct peaks can be seen at approximately 1610, 4550, and 7100 Hz. For the current transducer f_0 = 1534 Hz and one can see that the main frequency components in Figure 4.6 closely correspond to f_0, $3f_0$, and $5f_0$. It is noted from Figure 4.6 that the $3f_0$ peak has the strongest amplitude; such an observation seems to be a characteristic of the sound generated when spherical particles are present in the system [16]. It was obvious that the transducer behaved like an "organ pipe" [4] with one open end, the subharmonic frequencies have values that are odd multiples of the fundamental frequencies. The calculated fundamental frequency of the tested acoustic transducer as shown in Figure 2.1 confirmed this observation. The fundamental frequency for the transducer is given by $f_0 = c/4L$ where c is the speed of sound and L is the length of the column in this case it was 59.4 mm. The frequency content of the acoustic signals for different flow rates did not vary from that shown in Figure 4.6 for different flowrate. It appears that the spectral content of acoustic radiation closely depends on the geometry of the particle and transducer used.

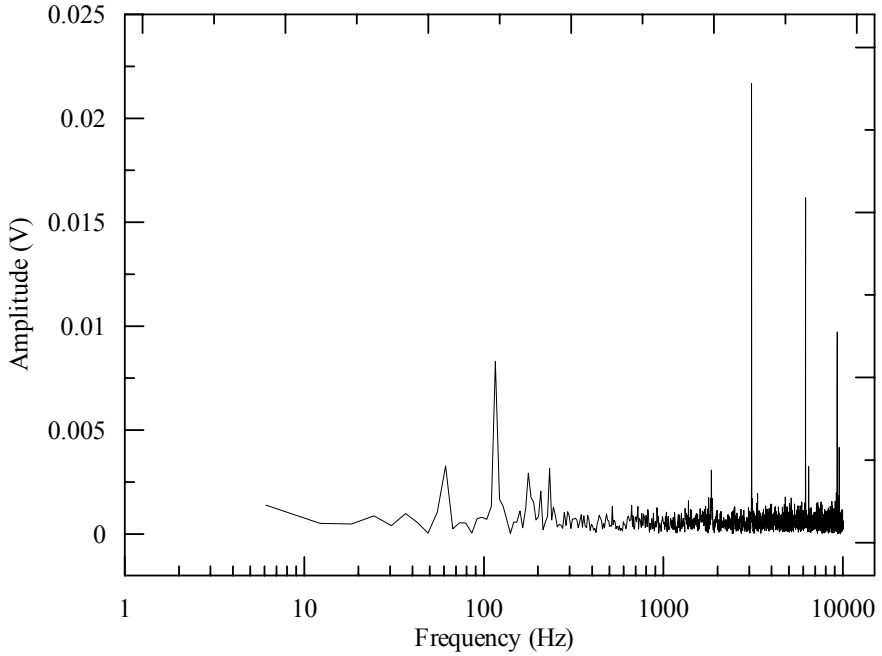

Figure 4.5: Frequency analysis of microphone signal when no particles are present.

When a wire (approx 250 μm in diameter) with a spherical tip at the end was placed in the transducer contraction, a continuous signal was generated as shown in Figure 4.7. The corresponding spectrum shown in Figure 4.8 was considerably different from the spectrum of the signals generated by the spherical particles. The fundamental peak strength is increased, and the amplitude at 7220 Hz is the highest; this seems to be a feature of elongated particles such as fibers [16]. Thus the frequency at which the signal peaks is seen to be a function of the transducer geometry.

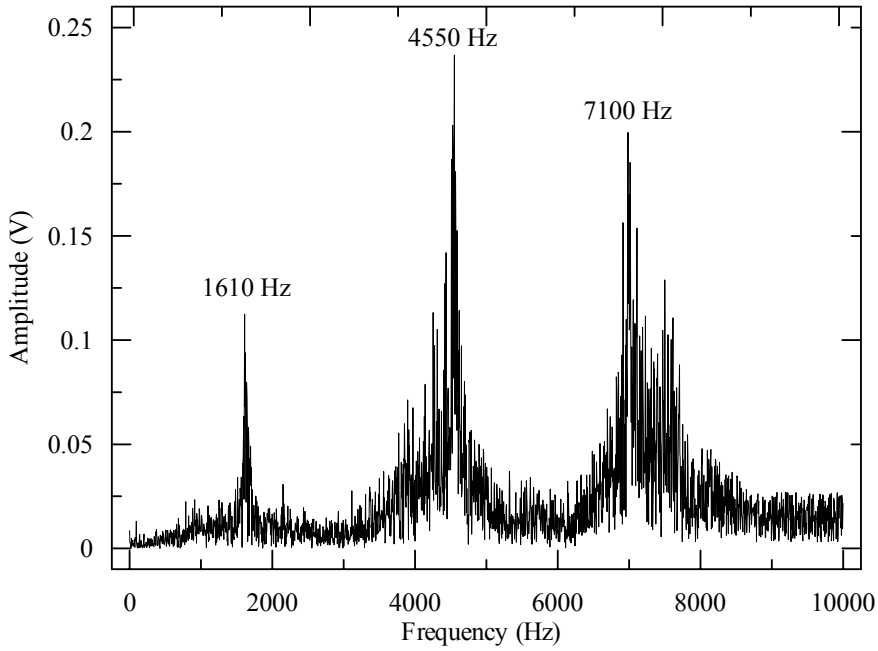

Figure 4.6: Frequency spectrum of acoustic signals for 50 Micron Particles at 40 L/min

Signal Strength

Mills and Chen speculated [4] that the strength of the acoustic signal would increase with the particle size, with the larger particles giving higher signal amplitude than the smaller ones. Mills and Chen [4] also speculated that the acoustic signal is possibly caused by either or both of two mechanisms: (1) the flow disturbance arising by the particle lag in the flow contraction with larger particles lagging the fluid motion more than smaller ones, (2) the unsteady particle motion in an accelerating flow field.

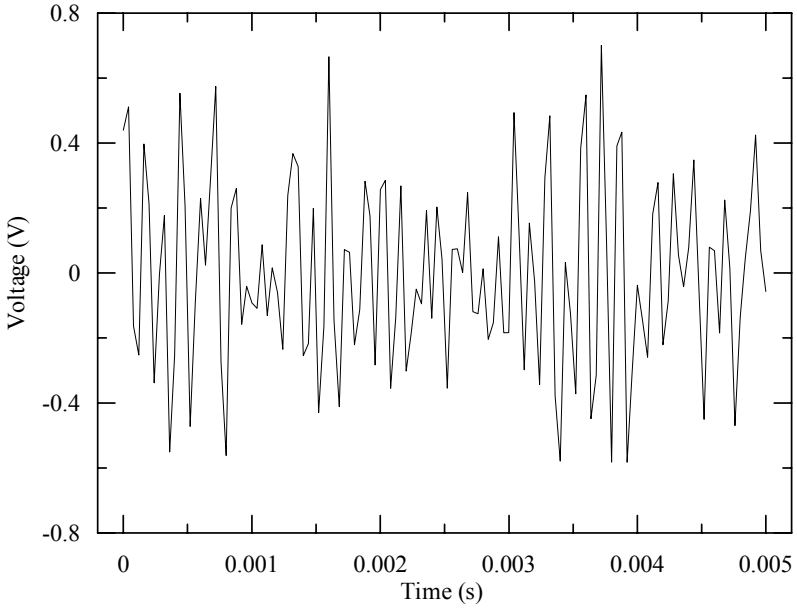

Figure 4.7: Acoustic signal when wire is placed in the transducer contraction.

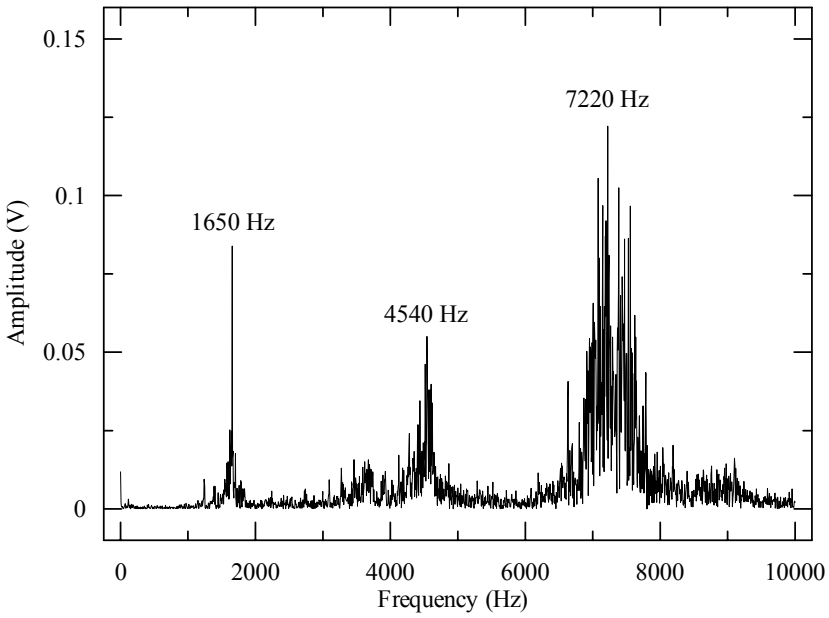

Figure 4.8: Frequency spectrum of signal in Figure 4.7.

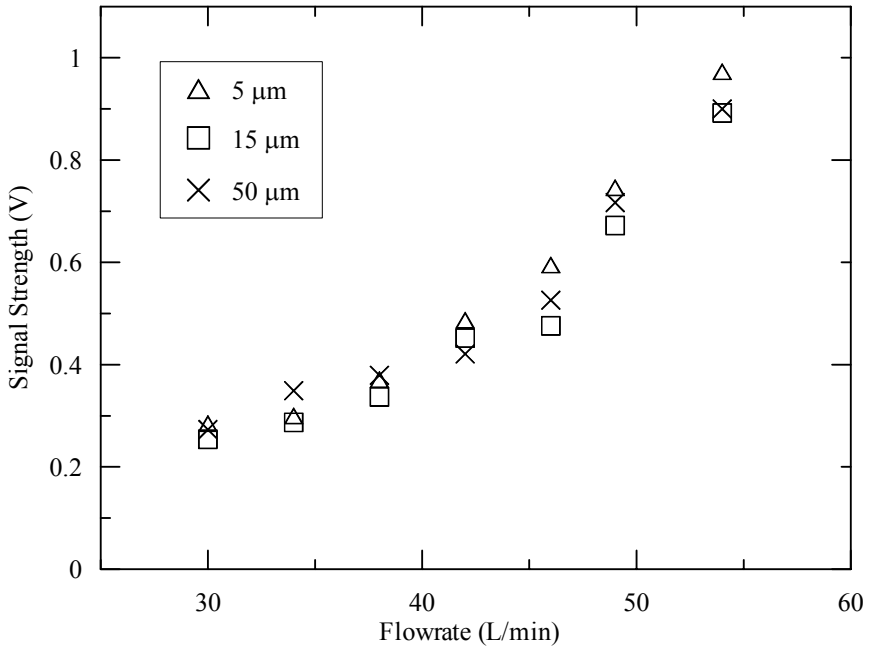

Figure 4.9: Peak-to-peak voltage vs. flowrate for different d_p.

To test this theory, PSL particles of 5 μm, 15 μm, and 50 μm were introduced in the system and the acoustic signal strength was measured for different flowrates. The size of the particles is controlled with deviations of ±6%, ±4%, and ±3% for 5 μm, 15 μm, and 50 μm sizes respectively [17]. As shown in Figure 4.9, no apparent variation in signal strength occurred with a change in particle size. For a given flowrate, acoustic signals were similar for all particle sizes tested. The amplitude of the signals varied considerably by ±20% of the average values shown in Figure 4.9.

As pointed out in Refs. [1-6], acoustic radiation generated by the transducer is perhaps due to the flow disturbance caused by the particles. In Refs. [1-3], however, radiation was attributed to the disturbance from shock wave phenomena. Shock waves

are not present here, since the pressure drop across the acoustic transducer was not sufficient to cause supersonic flow and create a shock wave. Chen *et al*. and co-workers [4-6] supported this result, and showed that the maximum Lagrangian acceleration of the flow occurs at the end of the contraction just prior to the capillary. With this result as motivation, the motion of the particles (as explained in the section related to the particle motion) in the contraction and the capillary section of the transducer were modeled numerically using a Runge-Kutta scheme by considering the acceleration imparted on the particles by the drag force due to the difference between air and particle velocities. Since air velocities can reach near sonic values for the flowrates considered in this experiment, air compressibility effects were included in the numerical model. The computational results are shown in Figure 4.10. For sizes greater than 2 μm, the particles never reach the airflow velocity. The maximum velocity difference occurs at the end of the contraction and it is at this location where the source of the acoustic signals is expected to originate [6]. Considering the Reynolds number based on the particle diameter (d_p) and the air-particle velocity difference at the end of the contraction yields values from 40 up to 600 for 2 μm < $d_p \leq$ 50 μm. In this regime an unsteady vortical wake is present downstream of the particles. This unsteady disturbance is expected to continue into the capillary altering the flow present in that section. Due to the high flow Reynolds number (in the order of 30,000) of the flow in the capillary, any small disturbance can induce the flow to become turbulent, thus generating noise amplified by the inlet section of the transducer. For particles smaller than 2 μm, the particle Reynolds numbers are always

less than 10 (i.e. near the creeping flow regime) and no wake develops downstream of the particles. Based on these results, the strength of the acoustic signals generated in the transducer is independent of particle size; particles big enough to induce turbulent flow in the capillary will generate signals. The Sound generated is again due to the flow alteration in the transducer capillary.

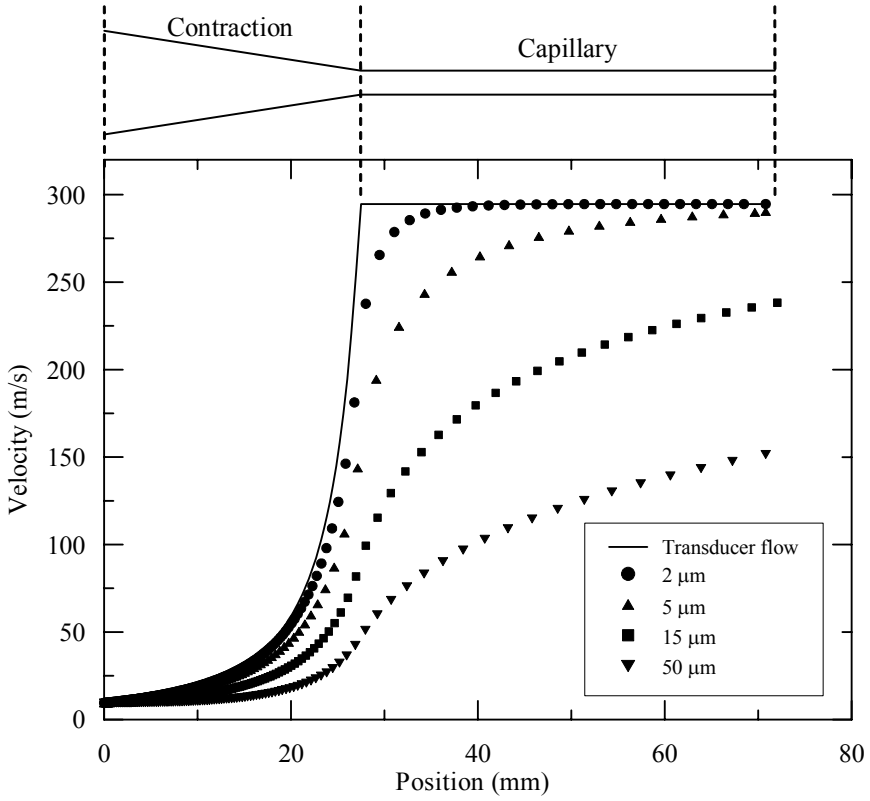

Figure 4.10: Particle velocities for a flowrate of 45 L/min.

Concentration

Previous studies [18] investigated the minimum detectable particle size and particle concentration with a similar acoustic transducer configuration but different length for the inlet section and the capillary section. The studies [18] reported differences of up to 40% between concentration measurements taken by the acoustic transducer and by the particle sizer.

The first test in this study was to evaluate the filter efficiency in removing airborne particles from the test chamber with the APS. When the filter is present, as shown in Figure 4.11, virtually no particles above 1 μm are present. Having the filter in the chamber reduces the concentration of particles below 1 μm by more than 60% when compared to the APS measurement when the inlet chamber is open to room air with no filter. Thus it is found that no naturally occurring particles in the inlet chamber will generate acoustic signals.

The second test was to correlate the particle concentration by the transducer and the particle sizer simultaneously. The inlet chamber was filled with spherical glass particles ranging in size from 1 μm to 20 μm, and several measurements were taken over a sampling time of 1 minute as the chamber was emptied by the vacuum pump. Figure 4.12 shows that concentration measurements from the APS and the transducer shows a linear relationship. However when comparing the measurements over the full range of the APS (0.5 to 20 micron), the transducer readings underestimate the APS concentration by more than 70%. For example for an APS reading of 600 ppl, the transducer only

measured 135 ppl for particles ranging from 0.5 to 2 micron in diameter. The correlation between the APS and the transducer improved when the concentration of particles larger than 2 micron was considered. In this case the transducer reading was within 15% of the APS readings. As discussed in the previous section, particles smaller than 2 μm are not expected to generate acoustic signals as they follow the changing air velocity through the contraction perfectly, and do not lead to flow disturbances. It is to be noted that the APS instrument can measure particles sizes between 0.5 μm and 20 μm with an accuracy of ±10%. The measurement suggest that the transducer was able to determine concentration lower than 2 ppl as Figure 4.12 shows.

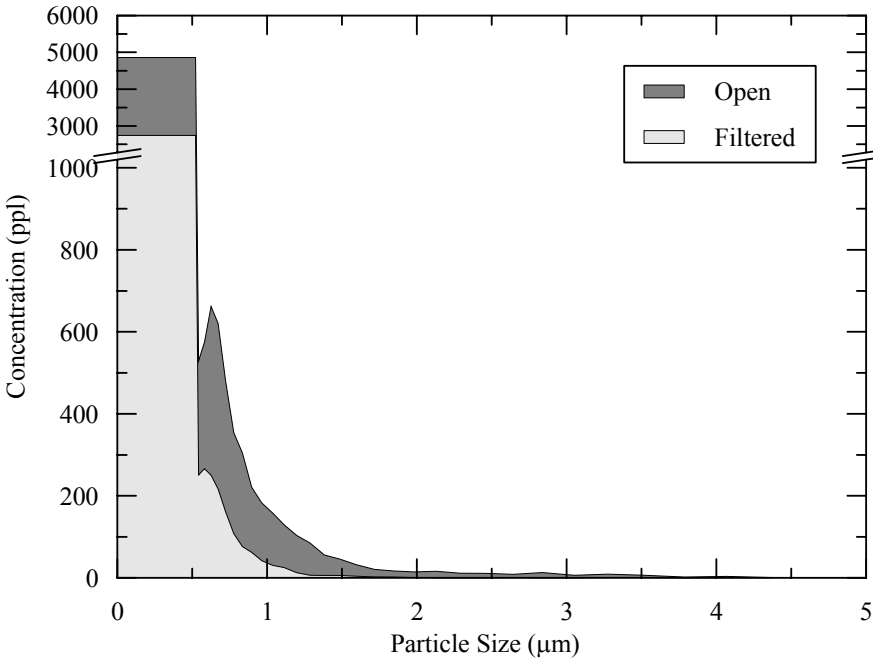

Figure 4.11: Concentration of naturally occurring particles inside the inlet chamber.

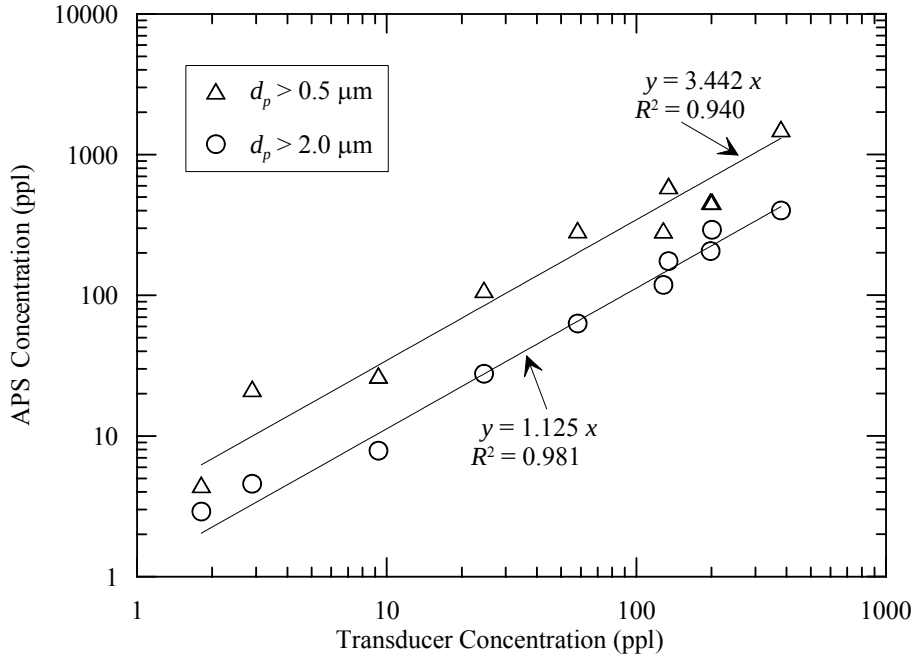

Figure 4.12: Concentration measurement comparison.

The maximum measurable concentration of the transducer as a function of flowrate was also evaluated. Figures 4.13 and 4.14 shows that the transducer can be very effective in measuring very dilute flows that can generate distinguishable signals. Figure 4.14 shows the trace or train of 4 particles with 5 micron diameter. Figure 4.13 indicates that the maximum concentration measurable by the transducer is only several hundred ppl. This makes the transducer ideal for concentration monitoring of high class clean rooms. For example, for a 10,000 class clean room, no more than 10,000 particles per cubic foot are allowed; this corresponds to approximately 350 ppl. The transducer concentration can be calculated by the following relationship $C = N_p / Q\, t_s$ where N_p is

the number of particles detected, Q is the flowrate and t_s is the sampling time. The maximum measurable concentration occurs when the microphone signal shows continuous acoustic signatures only separated by the time it takes the signals to decay. Assuming the signals decay within 3 ms (see Figures 4.2 – 4.4), Figure 4.13 shows the maximum measurable concentration to be always below 1,000 ppl for the range of flowrates used in this study.

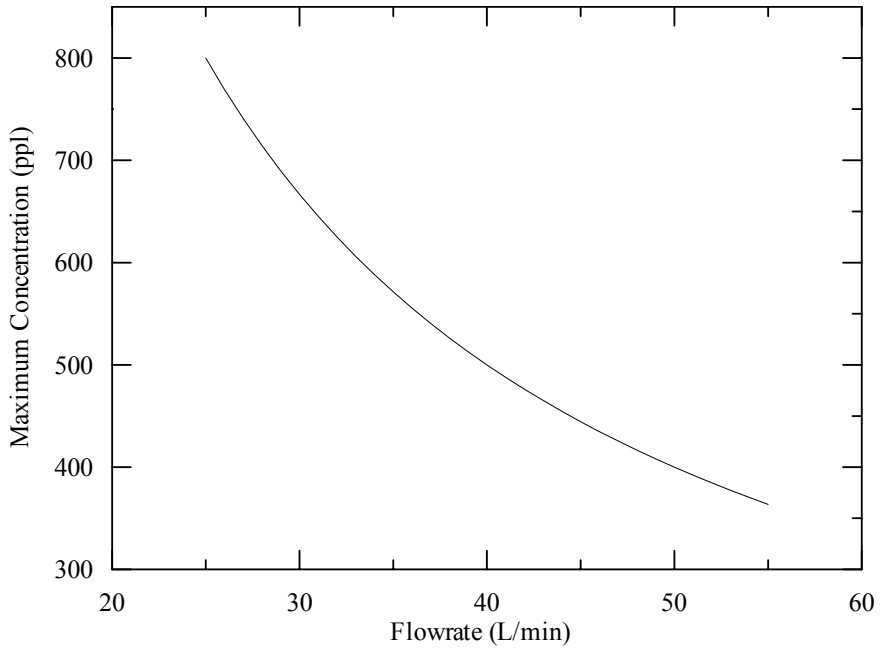

Figure 4.13: Expected maximum measurable concentration as a function of flow rate

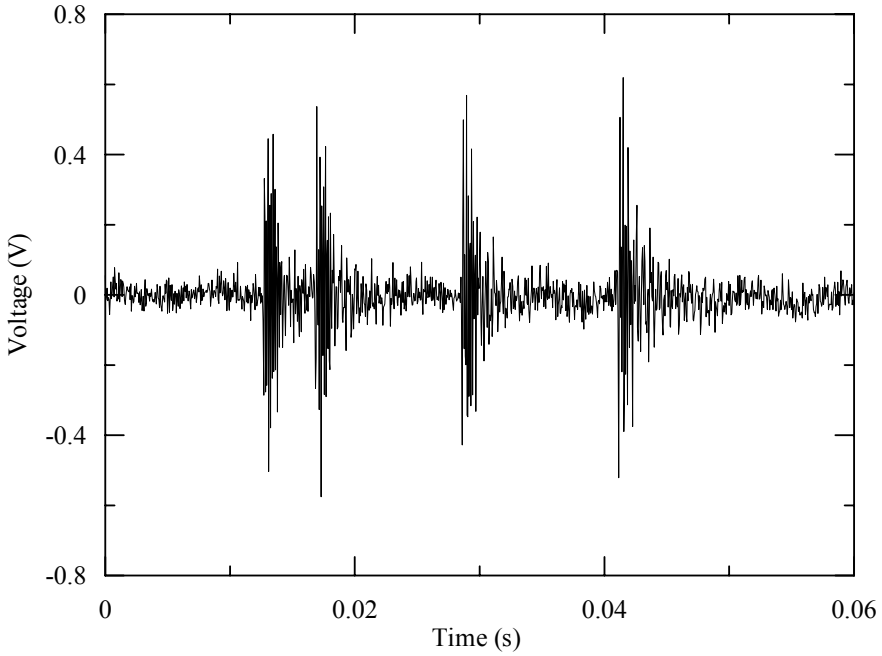

Figure 4.14: Signal train (5 μm PSL particles).

CHAPTER FIVE: CONCLUSION AND RECOMMENDATIONS

The concept of counting particles with an acoustic transducer has been demonstrated to be an effective method in detecting micron sized particles. With further testing and improvements the acoustic transducer could have applications in the aerospace, military and commercial sectors in the detection of aerosol particles in various clean room environments. The results obtained from this experiment support the fact that the acoustic signals are generated in the contraction section of the transducer due to the inability of the particles to follow the unsteady accelerating air flow around them and are not caused by the shock waves at the exit of the transducer. The difference between the particles and air velocities can cause an unsteady wake as the particles enter the transducer capillary disturbing the high Reynolds number flow at this location producing noise which is amplified by the inlet section of the transducer. The acoustic signal is comprised of resonant frequencies of the air column in the inlet section and, thus, is highly dependent on the transducer geometry.

No correlation was found to exist between particle size and the strength of the acoustic signals generated. It is thought that any unsteadiness present in the transducer capillary leads to a transition to turbulence in this section which is responsible for the acoustic radiation generated. Therefore, particles of sizes large enough to produce vortex or unsteady wakes will lead to acoustic signals.

The transducer was shown to be very capable of measuring concentration and one of its attractive features is the ability to measure low particle concentrations. However, with the current transducer tested no particles smaller than 2 μm can be detected.

Some of the recommendations that resulted from this experiment are:

1. Additional testing is recommended with different geometries for the acoustic transducer to investigate signal strength versus particle size and to determine whether larger particles could generate higher signal amplitude than smaller particles. It is recommended to construct an array of transducers with different contraction ratios and with various transition lengths between the inlet section and the capillary to evaluate the point above.
2. Further analytical investigation such as Computational Fluid Dynamics (CFD) is required to look at the particle-gas flow theory in the acoustic transducer and to better understand the physical process that causes the noise as particles travel in the contraction portion of the transducer and the possible transition to turbulent at the entrance region of the capillary.
3. Further investigation of the theory behind the acoustic power generation by particles in an accelerating flow field is also required. The relationship between sound power and particle velocity and diameter needs further investigation. The results from those investigations should provide theoretical backgrounds to further refine the system.

4. Further testing is recommended as well to evaluate the capabilities of the transducer in detecting the shape of the particles; that is to look at signal characteristics versus particle shape. A previous study [16] evaluated such a capability and showed that cylindrical fiber particles yield dominant peaks at frequencies different that those for spherical particles. The power spectra of the graphite fibers exhibited some discernible differences that may help in the identification of the shape of the aerosol particles.

With the above recommendations and further development, the transducer can improved so it can be used as a continuous air quality monitoring device in clean room or other applications as it involves no lasers and requires little power and can provide measurements comparable to those of more expensive systems.

APPENDIX A: AUTOCAD DRAWING SET

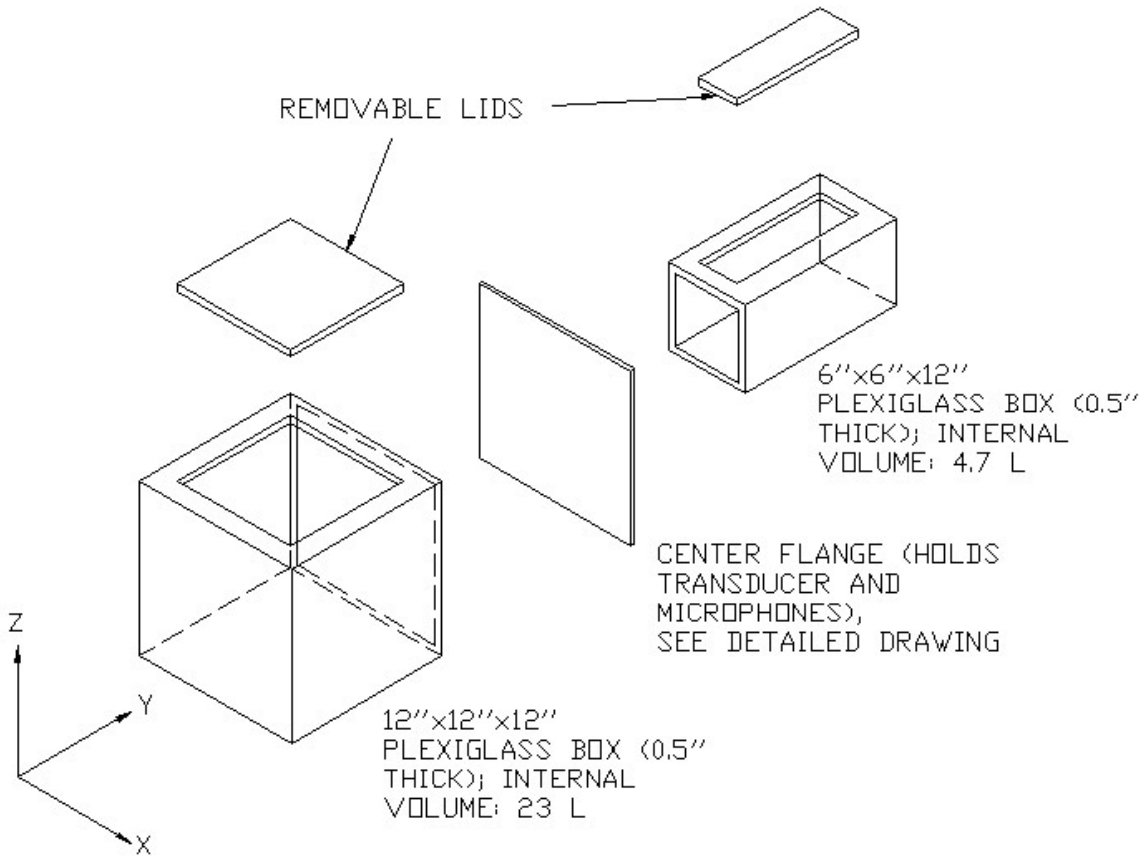
REMOVABLE LIDS
6''x6''x12''
PLEXIGLASS BOX (0.5''
THICK); INTERNAL
VOLUME: 4.7 L
CENTER FLANGE (HOLDS
TRANSDUCER AND
MICROPHONES),
SEE DETAILED DRAWING
Z
Y
X
12''x12''x12''
PLEXIGLASS BOX (0.5''
THICK); INTERNAL
VOLUME: 23 L

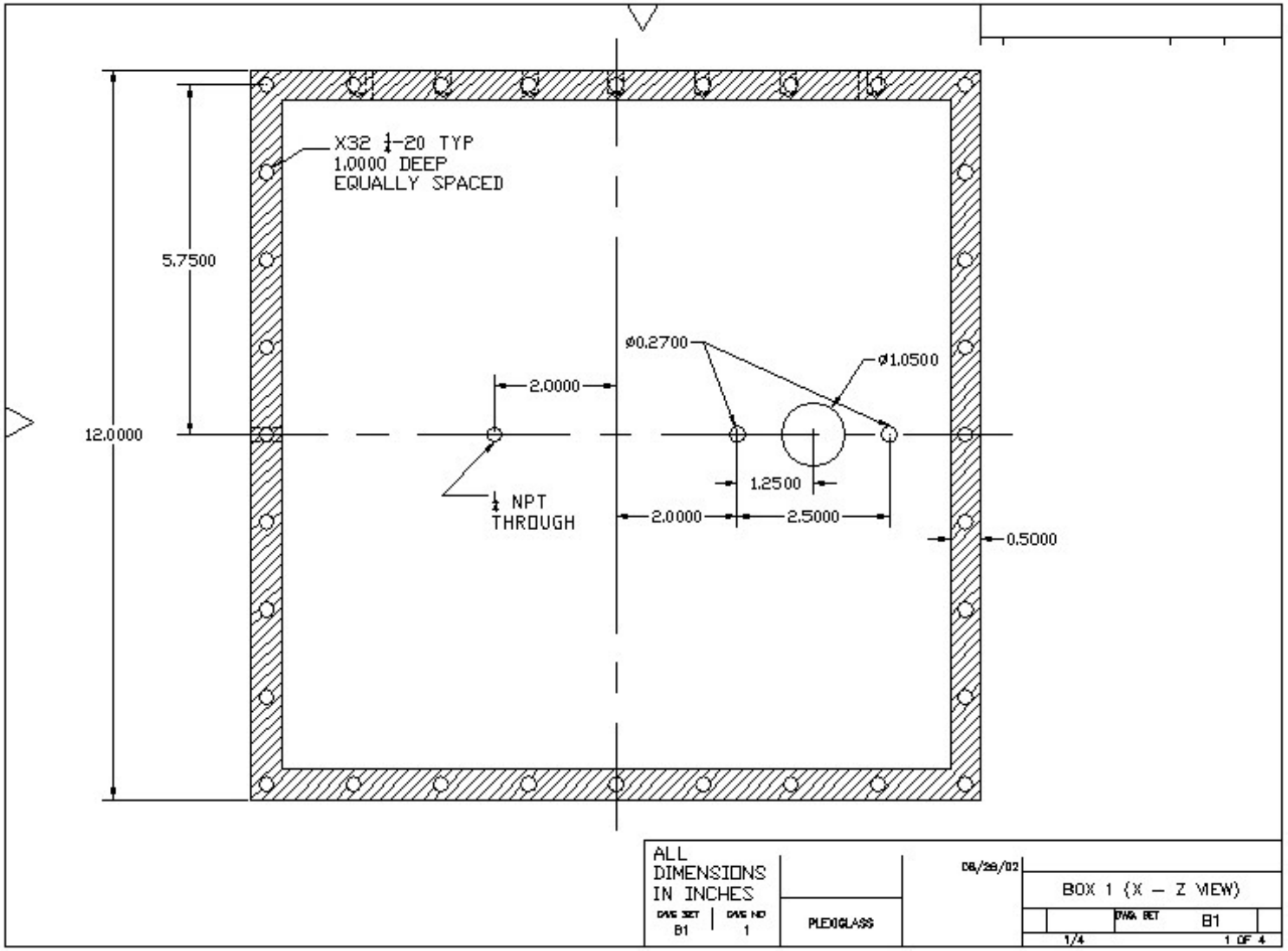
X32 ¼-20 TYP
1.0000 DEEP
EQUALLY SPACED
5.7500
12.0000
2.0000
ø0.2700
ø1.0500
¼ NPT
THROUGH
1.2500
2.0000
2.5000
0.5000
ALL
DIMENSIONS
IN INCHES
DWG SET
B1
DWG NO
1
PLEXIGLASS
08/29/02
BOX 1 (X – Z VIEW)
DWG SET
B1
1/4
1 OF 4

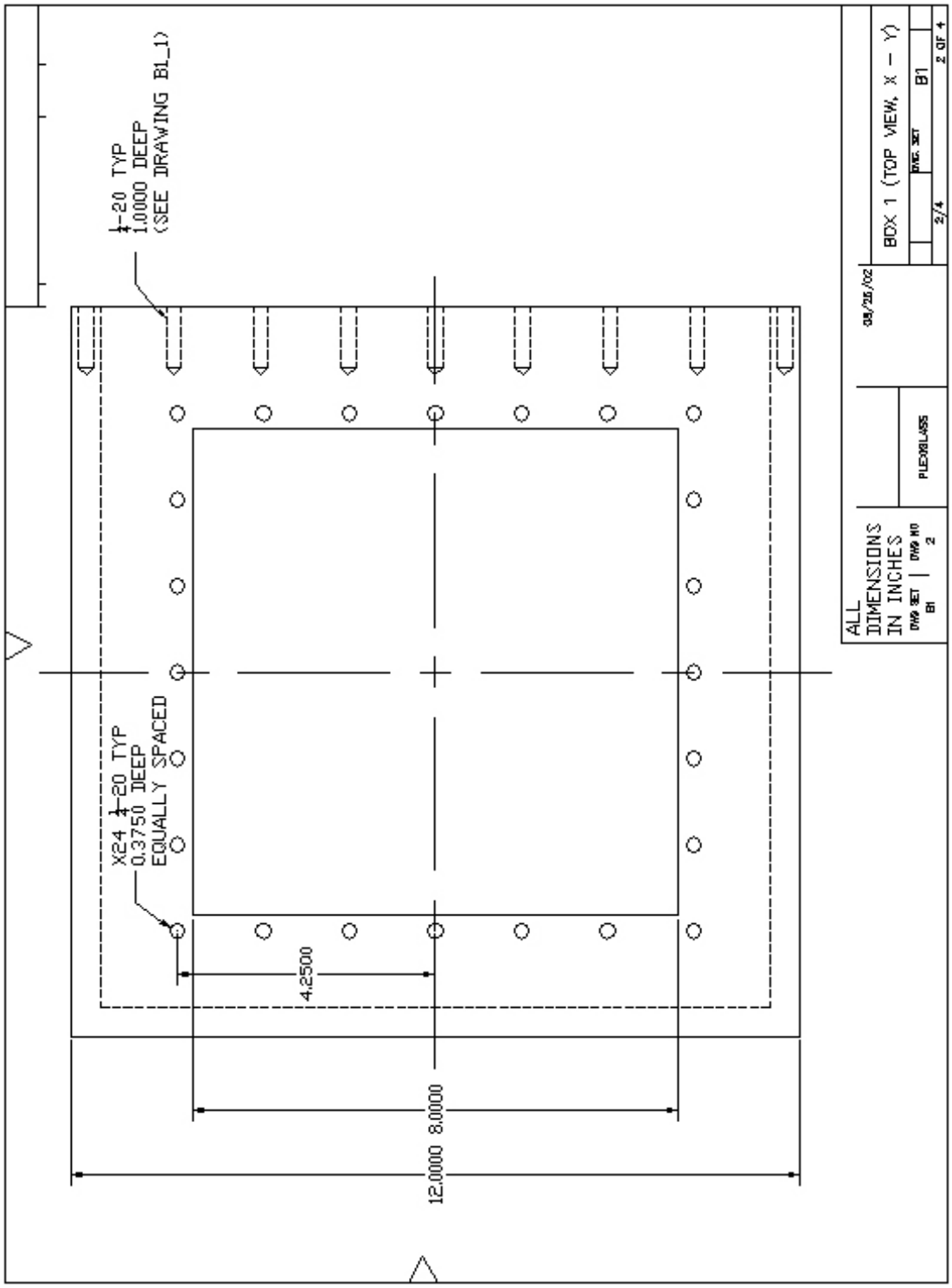
1/4-20 TYP
1.0000 DEEP
(SEE DRAWING B1_1)
X24 1/4-20 TYP
0.3750 DEEP
EQUALLY SPACED
4.2500
8.0000
12.0000
ALL
DIMENSIONS
IN INCHES
DWG SET | DWG NO
B1 2
PLEXIGLASS
08/25/02
BOX 1 (TOP VIEW, X - Y)
DWG SET B1
2/4
2 OF 4

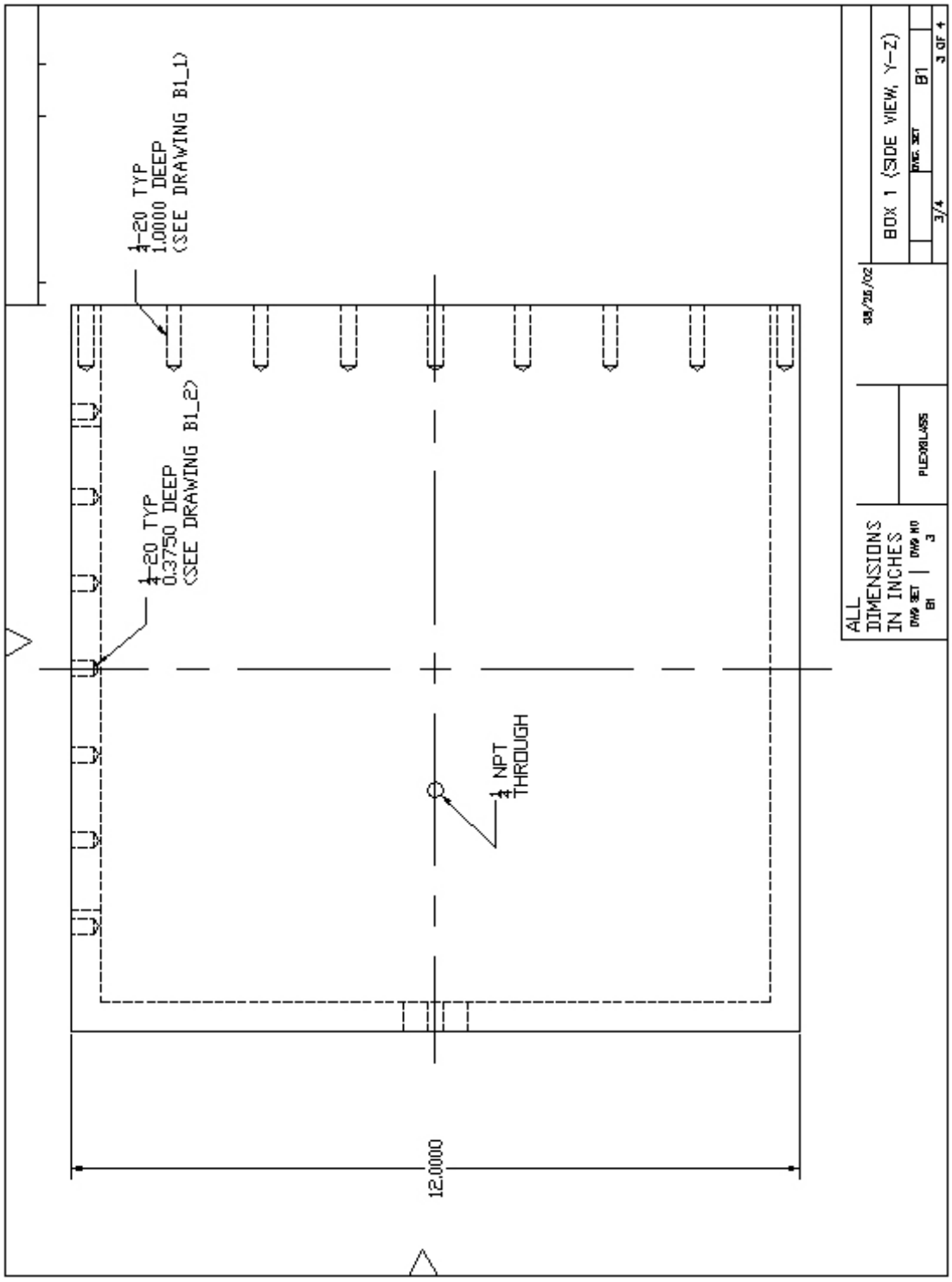
1/4-20 TYP
1.0000 DEEP
(SEE DRAWING B1_1)
1/4-20 TYP
0.3750 DEEP
(SEE DRAWING B1_2)
1/4 NPT
THROUGH
12.0000
ALL
DIMENSIONS
IN INCHES
DWG SET | DWG NO
B1 3
FLEXGLASS
03/25/02
BOX 1 (SIDE VIEW, Y-Z)
DWG SET B1
3/4
3 OF 4

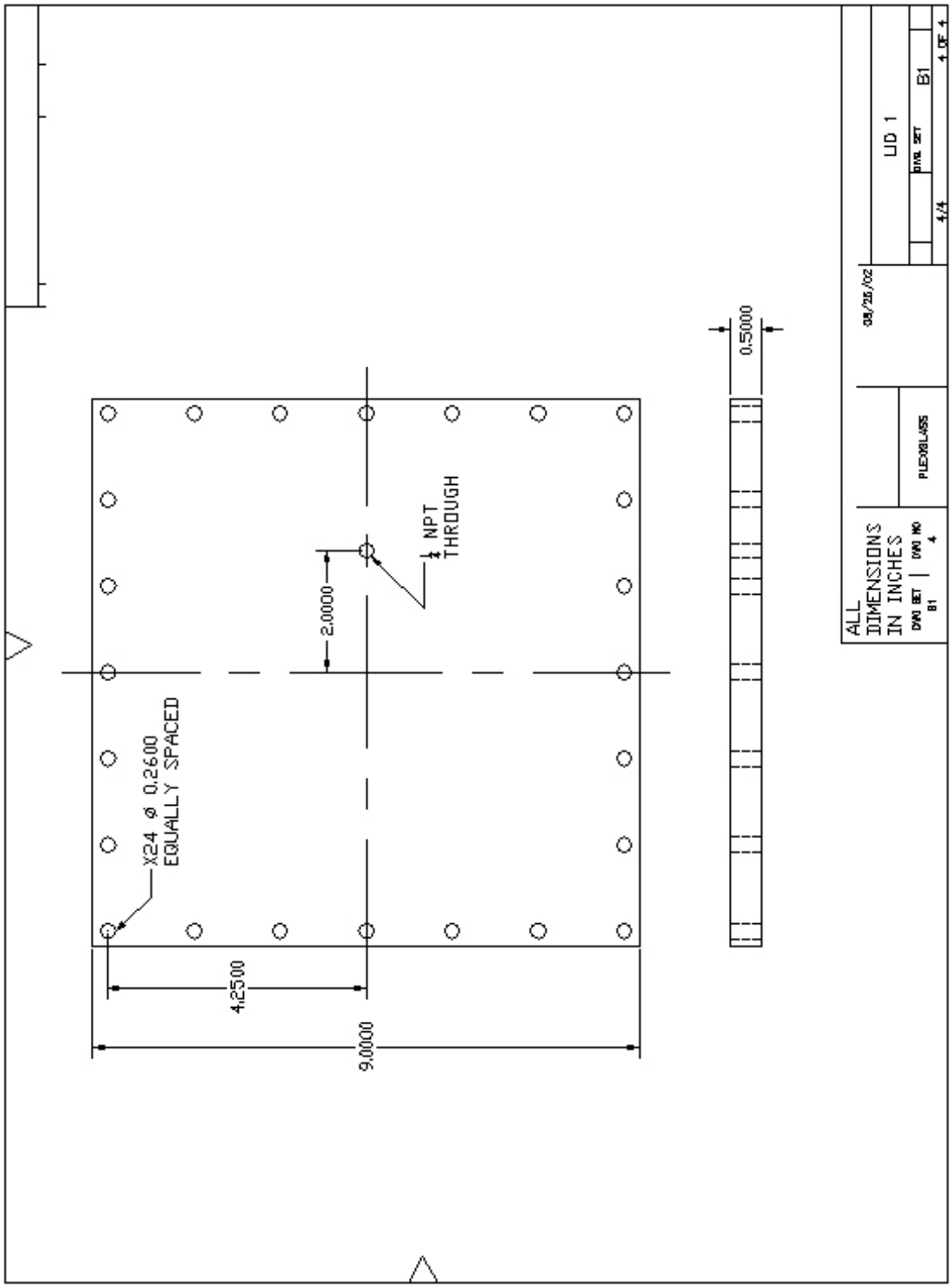
X24 ø 0.2600
EQUALLY SPACED
2.0000
NPT
THROUGH
4.2500
9.0000
0.5000
ALL
DIMENSIONS
IN INCHES
LID 1
B1
4/4
4 OF 4
PLEXIGLASS

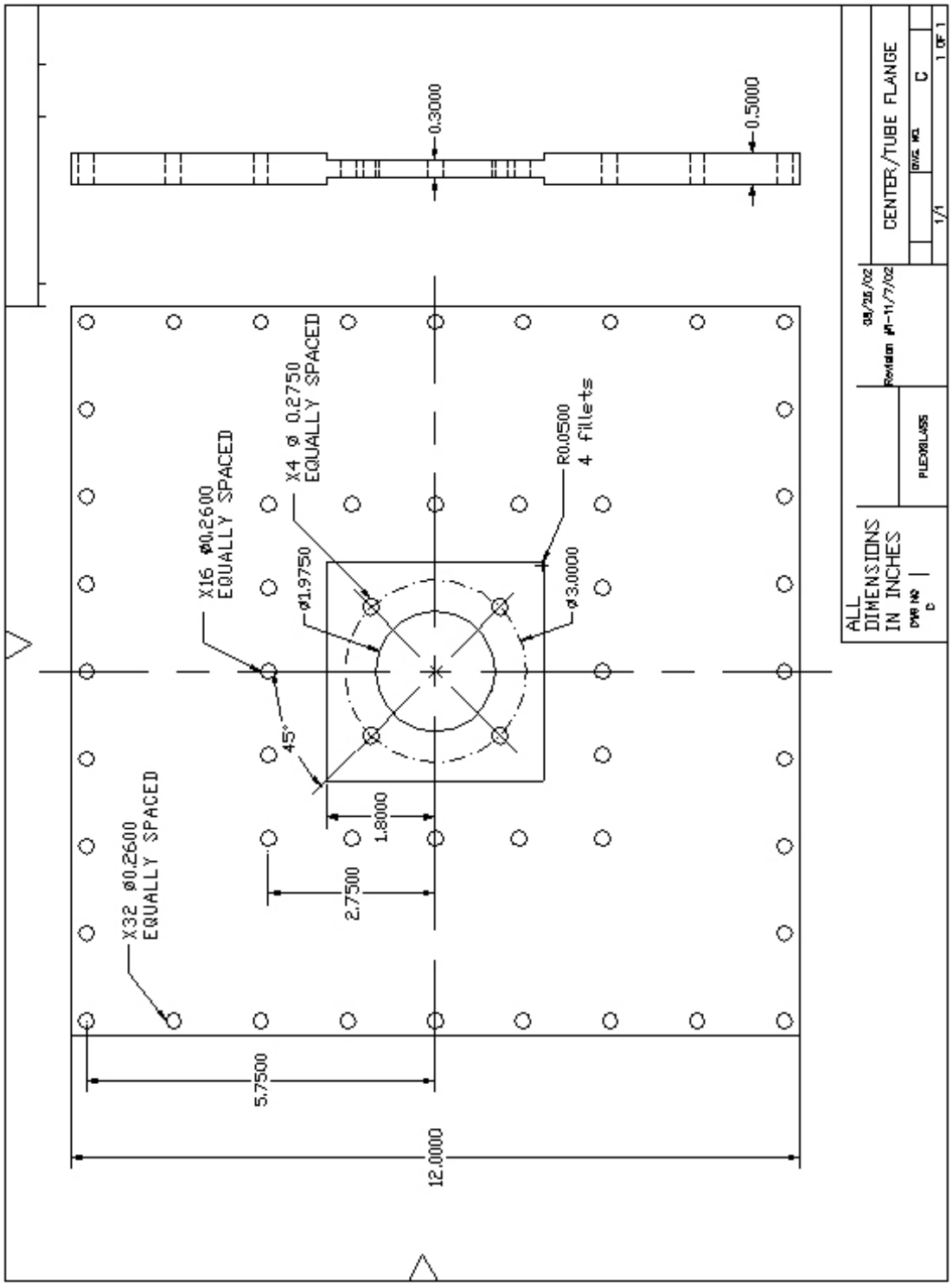
0.3000
0.5000
X16 ø0.2600
EQUALLY SPACED
X4 ø 0.2750
EQUALLY SPACED
R0.0500
4 fillets
ø1.9750
ø3.0000
45°
1.8000
2.7500
X32 ø0.2600
EQUALLY SPACED
5.7500
12.0000
ALL
DIMENSIONS
IN INCHES
DWG NO
B
FLEXGLASS
Revision #1-11/7/02
05/25/02
CENTER/TUBE FLANGE
DWG NO
C
1/1
1 OF 1

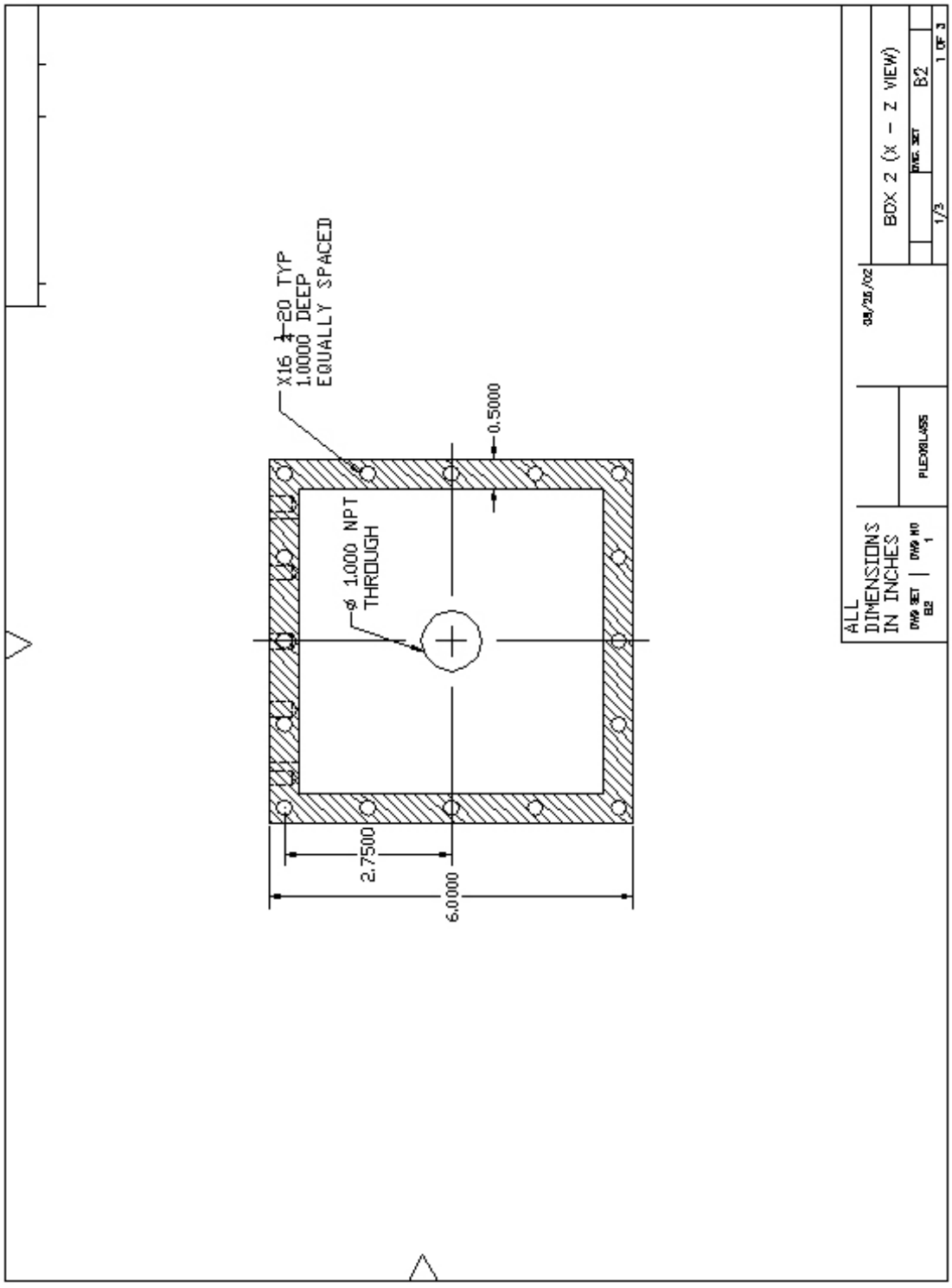
X16 1/4-20 TYP
1.0000 DEEP
EQUALLY SPACED
0.5000
ø 1.000 NPT
THROUGH
2.7500
6.0000
ALL
DIMENSIONS
IN INCHES
DWG SET | DWG NO
B2 1
PLEXIGLASS
05/25/02
BOX 2 (X - Z VIEW)
DWG. SET B2
1/3
1 OF 3

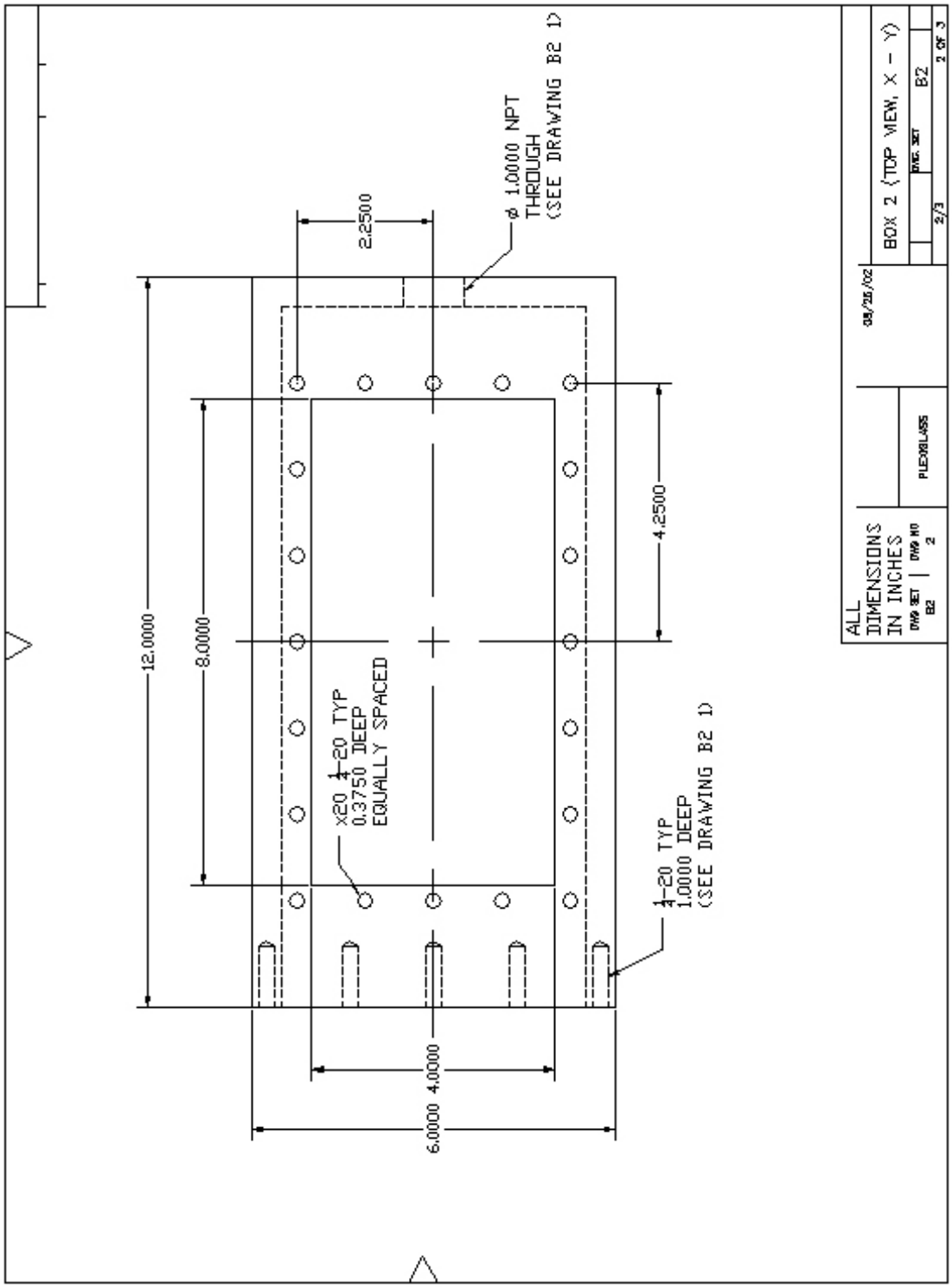
ALL DIMENSIONS IN INCHES
DWG SET | DWG NO
B2 2
PLEXIGLASS
08/25/02
BOX 2 (TOP VIEW, X - Y)
DWG SET B2
2/3
2 OF 3
ø 1.0000 NPT THROUGH (SEE DRAWING B2 1)
2.2500
4.2500
12.0000
8.0000
x20 ¼-20 TYP 0.3750 DEEP EQUALLY SPACED
¼-20 TYP 1.0000 DEEP (SEE DRAWING B2 1)
4.0000
6.0000

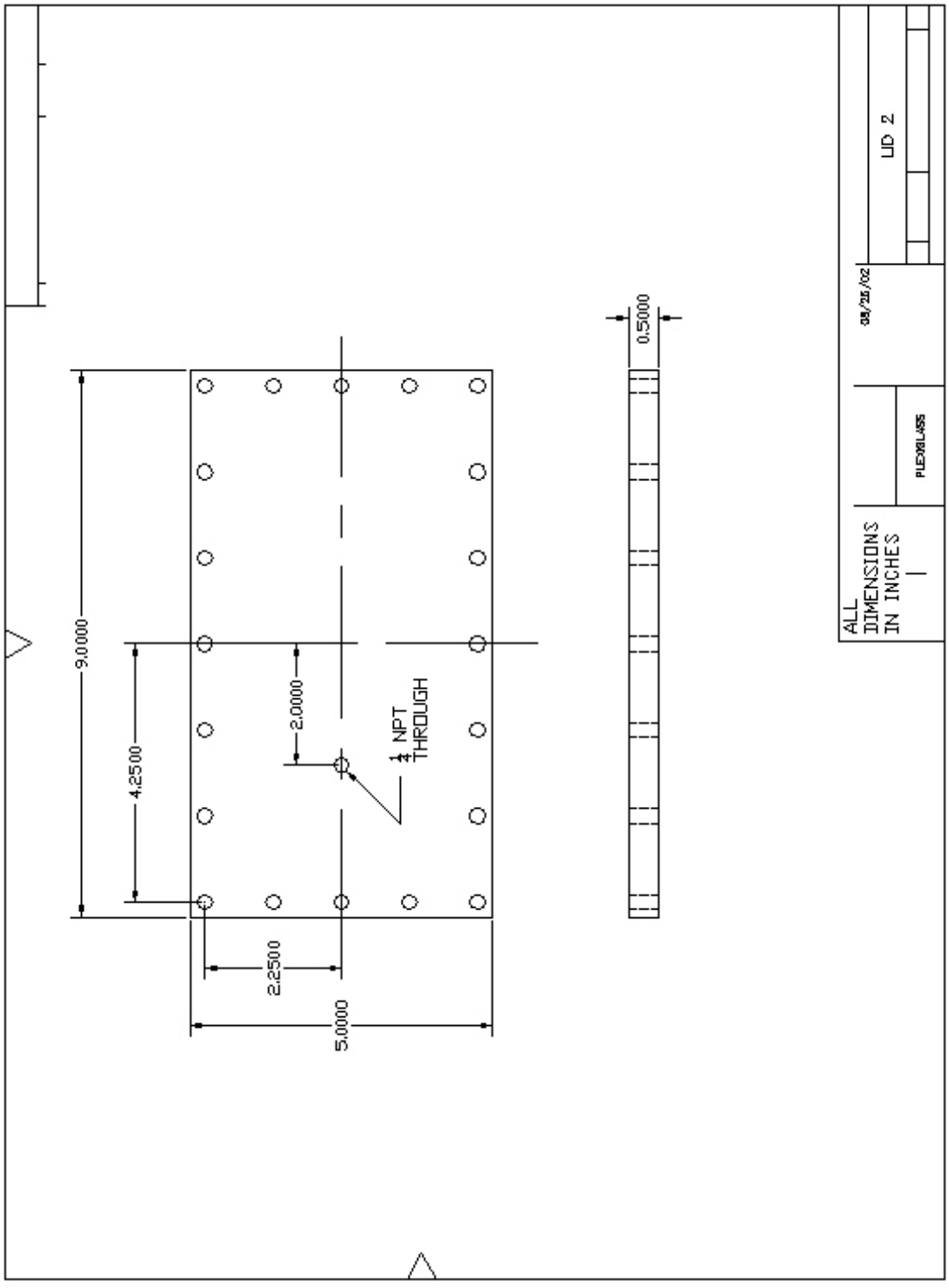
9.0000
4.2500
2.0000
1/4 NPT
THROUGH
2.2500
5.0000
0.5000
ALL
DIMENSIONS
IN INCHES
PLEXIGLASS
LID 2

APPENDIX B: LABVIEW DIAGRAMS

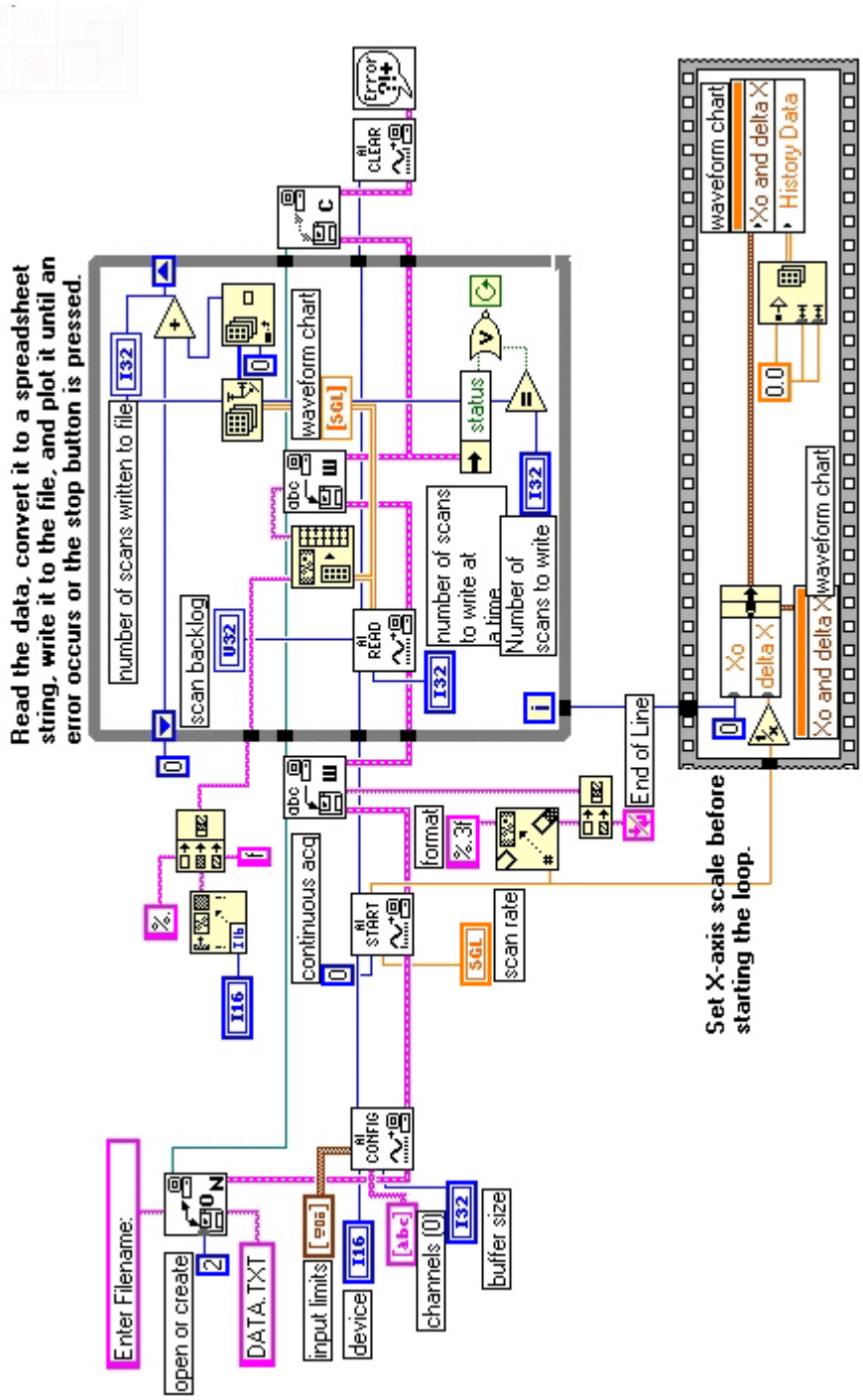
Read the data, convert it to a spreadsheet string, write it to the file, and plot it until an error occurs or the stop button is pressed.
Set X-axis scale before starting the loop.
Enter Filename:
open or create
DATA.TXT
input limits
device
channels [0]
buffer size
continuous acq
scan rate
format
%.3f
End of Line
number of scans written to file
scan backlog
waveform chart
status
number of scans to write at a time
Number of scans to write
Xo
delta X
Xo and delta X
History Data
0.0

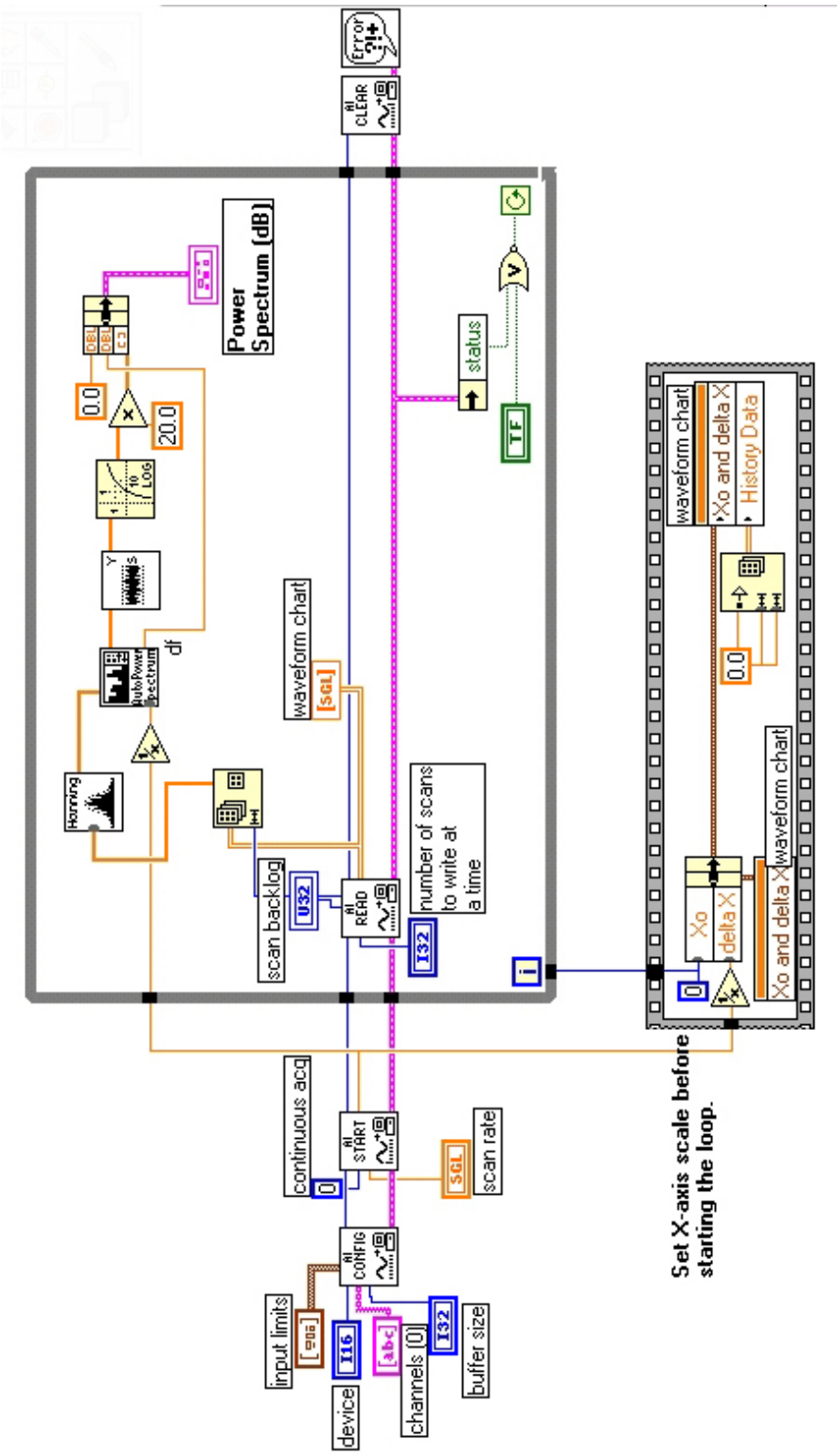
Power Spectrum (dB)
df
Hanning
waveform chart
scan backlog
number of scans to write at a time
status
continuous acq
scan rate
input limits
device
channels (0)
buffer size
Xo
delta X
Xo and delta X
waveform chart
Xo and delta X
History Data
Set X-axis scale before starting the loop.

APPENDIX C: FORTRAN PROGRAMS FOR DATA ANALYSIS

```
      PROGRAM PART_VEL
************************************************************************
*                                                                      *
* Date:     12/16/04                                                   *
*                                                                      *
* Task:     This program calculates particle velocity as it moves      *
*           through an accelerating viscous medium.  It is assumed     *
*           that the only force on the particle is the drag force due  *
*           to the velocity difference between the particle and        *
*           surrounding flow.  This assumption turns this problem into *
*           a simple 1-D case.  The particle velocity and position is  *
*           solved for using a 4th order Runge-Kutta algorithm.  Air   *
*           compressibility is taken into account when calculating the *
*           drag force on the spherical particle.                      *
*                                                                      *
* Input:    User inputs the geometric parameters that confine the flow *
*           (i.e. inlet and capillary diameters of the acoustic        *
*           transducer); as well the system flowrate, particle size    *
*           and density.                                               *
*                                                                      *
* Output:   The program writes to a file named "output.txt" 5 columns: *
*           time, position within the transducer, particle velocity,   *
*           particle acceleration, and airflow velocity.               *
*                                                                      *
* Major                                                                *
* Variables:POS,VEL,ACC,TIM,AIR - Arrays containing output data        *
*           Accel - Function that calculates particle acceleration at  *
*                   a given position within the transducer.            *
*           x,v,dx1,dv1,dx2                                            *
*           dv2,dx3,dv3,dx4,dv4 - Intermediate variables used to       *
*                                 update particle velocity and         *
*                                 position through the Runge-Kutta     *
*                                 scheme.                              *
*                                                                      *
************************************************************************

         IMPLICIT NONE

         REAL*8, PARAMETER :: PI=3.1415926535898
         INTEGER, PARAMETER :: N=1000000
         INTEGER I,K
         REAL*8 Q,d1,d2,dp,Lcn,Lcp,rho_PSL,t,t_step
         REAL*8 POS(N),VEL(N),ACC(N),TIM(N),AIR(N),x,v,a,Accel
         REAL*8 dx1,dv1,dx2,dv2,dx3,dv3,dx4,dv4

      ! User inputs
         WRITE (*,*) 'Enter system flowrate (L/min):'
         READ (*,*) Q

         WRITE (*,*) 'Enter transducer inlet diameter (mm):'
         READ (*,*) d1

         WRITE (*,*) 'Enter transducer capillary diameter (mm):'
         READ (*,*) d2

         WRITE (*,*) 'Enter contraction length (mm):'
         READ (*,*) Lcn

         WRITE (*,*) 'Enter capillary length (mm):'
```

```
   READ (*,*) Lcp

   WRITE (*,*) 'Enter particle diameter (microns):'
   READ (*,*) dp

   WRITE (*,*) 'Enter particle density (g/cm^3):'
   READ (*,*) rho_PSL

! Transform to SI units
   Q=Q/60000
   d1=d1/1000
   d2=d2/1000
   Lcn=Lcn/1000
   Lcp=Lcp/1000
   dp=dp/1000000
   rho_PSL=rho_PSL*1000

! Since adaptive step-sixe algoriths will not be used, calculate
! the time it takes for the airflow to move through the
! contraction; divide this time into 100 equal time steps to
! provide good resolution for the calculation. Note: this 100
! value may have to be changed for very small particle sizes.
   t=PI*Lcn*(d1**2+d1*d2+d2**2)/(12*Q)
   t_step=t/100

! Array initialization
   I=1
   POS(I)=0.0
   VEL(I)=4*Q/(PI*(d1**2))
   ACC(I)=0.0
   TIM(I)=0.0

! Apply the Runge-Kutta time marching scheme while the particle
! is inside the contraction or the capillary. At each position,
! the particle acceleration is calculated from the drag force
! based on the velocity slip between the particle and the
! surrounding airflow by calling a function
   DO WHILE (POS(I).LT.(Lcn+Lcp))
      !Calculate airflow speed at given position
      IF (POS(I).LE.Lcn) THEN
         AIR(I)=(4*Q/PI)/((d1-(d1-d2)*POS(I)/Lcn)**2)
      ELSE
         AIR(I)=(4*Q/PI)/(d2**2)
      END IF

      x=POS(I)
      v=VEL(I)

      dv1=t_step*Accel(x,v,Q,d1,d2,Lcn,dp,rho_PSL)
      dx1=t_step*v

     dv2=t_step*Accel(x+0.5*dx1,v+0.5*dv1,Q,d1,d2,Lcn,dp,rho_PSL)
      dx2=t_step*(v+0.5*dv1)

     dv3=t_step*Accel(x+0.5*dx2,v+0.5*dv2,Q,d1,d2,Lcn,dp,rho_PSL)
      dx3=t_step*(v+0.5*dv2)

      dv4=t_step*Accel(x+dx3,v+dv3,Q,d1,d2,Lcn,dp,rho_PSL)
      dx4=t_step*(v+dv3)
```

```
            I=I+1
            POS(I)=POS(I-1)+(dx1+2*dx2+2*dx3+dx4)/6
            VEL(I)=VEL(I-1)+(dv1+2*dv2+2*dv3+dv4)/6
            ACC(I)=Accel(POS(I),VEL(I),Q,d1,d2,Lcn,dp,rho_PSL)
            TIM(I)=TIM(I-1)+t_step

         END DO

         OPEN (10,FILE='output.txt')
         WRITE (10,'("Particle size: ",F4.1," microns")') (dp*1000000)
         WRITE (10,'("Flowrate:",F6.2," L/min")') (Q*60000)
         WRITE (10,'("Inlet diameter: ",F4.1," mm")') (d1*1000)
         WRITE (10,'("Capillary diameter: ",F4.1," mm")') (d2*1000)
         WRITE (10,'("Contraction length: ",F4.1," mm")') (Lcn*1000)
         WRITE (10,'("Capillary length: ",F4.1," mm",/,/)') (Lcp*1000)
         WRITE (10,'(5X,"t(s)",13X,"x(mm)",11X,"v(m/s)",10X,"a(m/s2)",
     $             8X,"air vel (m/s)")')
         WRITE (10,'(5("--------------",3X))')

         DO K=1,I
            WRITE (10,'(5(E14.8,3X))') TIM(K),POS(K)*1000,VEL(K),ACC(K)
     $                                 ,AIR(K)
         END DO
       END

!-----------------------------------------------------------------------
       ! The following function computes the acceleration of the
       ! particle in the accelerating viscuos medium.  Only the
       ! instantaneous drag force is considered, added mass and wave
       ! drag as well as buoyancy are neglected.

       REAL*8 FUNCTION Accel(x,v,Q,d1,d2,Lcn,dp,rho_PSL)
      $        RESULT (acceleration)

         ! Air viscosity and density at 20C and 1 atm, (Ns/m^2;kg/m^3)
         REAL*8, PARAMETER :: visc_0=1.8417E-5
         REAL*8, PARAMETER :: rho_0=1.2041

         REAL*8, PARAMETER :: PI=3.1415926535898
         REAL*8 x,v,Q,d1,d2,Lcn,dp,rho_PSL
         REAL*8 Vf,Re,M,rho_air,kvisc_air,Cd

         ! Calculate fluid velocity as function of position within the
         ! transducer
         IF (x.LE.Lcn) THEN
            Vf=(4*Q/PI)/((d1-(d1-d2)*x/Lcn)**2)
         ELSE
            Vf=(4*Q/PI)/(d2**2)
         END IF

         ! Reynolds number calculation; The viscosity of air is assumed
         ! constant but the air density is modified by employing
         ! compressible flow relations.  The calculated air density is
         ! Used to calculate the kinematic viscosity of air which, in
         ! turn, is used to calculate the Reynolds number.
         M=Vf/SQRT(1.4*287.0*293.15)           !Mach number
         rho_air=rho_0/((1+0.2*(M**2))**(2.5)) !air density for given M
         kvisc_air=visc_0/rho_air              !kinematic air viscosity
```

```
   Re=(Vf-v)*dp/kvisc_air

   ! Drag Coefficient using the expressions of Stokes, Osteen and
   ! Clift for the different flow regimes.
   IF (Re.LE.0.0) THEN
      Cd=0.0
   ELSE IF (Re.LE.0.5) THEN
      Cd=24.0/Re
   ELSE IF (Re.LE.1.0) THEN
      Cd=24*(1+3*Re/16)/Re
   ELSE IF (Re.LE.1000.0) THEN
      Cd=24*(1+0.15*(Re**0.687))/Re
   ELSE
      Cd=0.44
   END IF

   acceleration=3*Cd*rho_air*((Vf-v)**2)/(4*rho_PSL*dp)

   RETURN

END FUNCTION
```

```
      PROGRAM PEAK
************************************************************************
*                                                                      *
* Date:     11/8/04                                                    *
*                                                                      *
* Task:     This program reads a raw data file containing microphone   *
*           voltage readings and searches for acoustic signals         *
*           generated by particles to determine the peak-to-peak       *
*           voltage of the signals.  The user has the option to        *
*           determine threshold values for particle detection either   *
*           through direct keyboard input or by inputting a data file  *
*           containing microphone voltage data taken without any       *
*           particles present in the system.  After the program finds  *
*           a value that exceeds the threshold values set by the user, *
*           it searches for the maximum and minimum voltages within an *
*           envelope of data points, also user determined.  The        *
*           programs performs this task in an iterative manner until   *
*           the input file has been analyzed entirely.  In addition,   *
*           the program also calculates the particle concentration in  *
*           the sample based on the user-supplied sample flowrate      *
*           value.                                                     *
*                                                                      *
* Input:    The program asks for the raw data file to be analyzed and  *
*           the user can provide this interactively.                   *
*                                                                      *
* Output:   The program outputs (to a user-specified file) the set     *
*           threshold values, the data envelope, the number of         *
*           particles detected (if any) and the peak-to-peak voltage   *
*           values along with the data index the signals are found at. *
*                                                                      *
* Major                                                                *
* Variables:ANSWER - Stores answer given by user when asked source of  *
*                    threshold values.                                 *
*           DAT - Array that stores signal data                        *
*           CONC - Particle concentration (ppl) in the sample          *
*           ENVLP - Number of data points forming the signal envelope  *
*                   (user defined)                                     *
*           FILEDAT - Stores input (data) file name (user defined)     *
*           FILENM - Stores input file name of threshold file (user    *
*                    defined)                                          *
*           FILEOUT - Stores output file name (user defined)           *
*           FLOW - Sample flowrate (L/min, user defined)               *
*           INDX - Array containing the index values where found       *
*                  signals start                                       *
*           PP - Array where calculated peak-to-peak values are stored *
*           STIM - Sampling time, i.e. ratio of number of points in    *
*                  DAT array and sampling rate (first value in DAT     *
*                  array)                                              *
*           SUBARR - Array of signal envelope                          *
*           T - Array where threshold file data is stored              *
*           THRSMIN, THRSMAX - Minimum and Maximum threshold values    *
*           SUM,SUMSQ,AVG,STDEV,SD - Variables that help calculate     *
*                                    average and standard deviation of *
*                                    threshold file                    *
************************************************************************


      PARAMETER (NMAX=3000000)
      CHARACTER ANSWER,FILEDAT*12,FILEOUT*12,DONE*3
```

```
      INTEGER I/1/,J/0/,K,L,N/0/,ENVLP,INDX(NMAX)
      LOGICAL ANSWERING/.TRUE./,UNSORTED/.TRUE./
      REAL*8 THRSMIN,THRSMAX,DAT(NMAX),SUBARR(NMAX),PP(NMAX)
      REAL*8 FLOW,STIM,CONC,SUM,AVG,TEMP

   ! Ask user for threshold values (whether from keyboard or
   ! microphone data file taken without any particles flowing
   ! through the transducer). If a file is selected to provide
   ! threshold values, a subroutine is called that calculates the
   ! mean and standard deviation of the data in the file and sets
   ! the threshold values according to how many standard deviations
   ! away from the mean the user wants these values to be.
      WRITE (*,*)'Would you like to use a file to set the'
     $             ' threshold values? (Y/N)' ! Answer can be upper or
                                              ! lowercase
      READ (*,*) ANSWER

      DO WHILE (ANSWERING)
         IF ((ANSWER.EQ.'N') .OR. (ANSWER.EQ.'n')) THEN
            ANSWERING=.FALSE.
            WRITE (*,*) 'Enter threshold mimimum:'
            READ (*,*) THRSMIN
            WRITE (*,*) 'Enter threshold maximum:'
            READ (*,*) THRSMAX
         ELSE
            IF ((ANSWER.EQ.'Y') .OR. (ANSWER.EQ.'y')) THEN
               CALL THRSHOLD (THRSMIN,THRSMAX) ! calls the
                                               ! subroutine
               ANSWERING=.FALSE.
            ELSE
               WRITE (*,*) 'You must answer "Y(y)" for yes',
     $                     ' or "N(n)" for no.'
               READ (*,*) ANSWER
            END IF
         END IF
      END DO

   ! Ask for file names: output and input (containing the particle
   ! signals)
      WRITE (*,*) 'Enter output file name (include file extension,',
     $            ' 12 characters maximum):'
      READ (*,*) FILEOUT

      WRITE (*,*) 'Enter signal data (input) file name (include',
     $            ' file extension, 12 characters maximum):'
      READ (*,*) FILEDAT

   ! Ask for signal envelope (typically a signal decays within 3 ms,
   ! for a data rate of 20,000 Hz this would correspond to an
   ! envelope of 60 data points)
      WRITE (*,*) 'Enter number of points to search for peak-to-',
     $            'peak determination after a signal is detected:'
      READ (*,*) ENVLP

   ! Sampling flowrate
      WRITE (*,*) 'Enter sampling flowrate (L/min):'
      READ (*,*) FLOW
```

```
! Open and read input data file
   OPEN     (10,FILE=FILEDAT)
   DO WHILE (.NOT. EOF(10))
      N=N+1
      READ (10,*) DAT(N)
   END DO
   CLOSE (10)


! The data file is searched for points that exceed (or are below)
! the set threshold values. Once such point is found, a subarray
! is formed containing all the data within the envelope set by
! the user. The maximum and minimum values of this subarray are
! calculated and the difference between them is the maximum peak
! to-peak voltage generated by the particle. The index (point at
! which the signal starts) is also stored so that, if needed, the
! signal can be found in the raw data file
   DO WHILE (I.LT.N)
      I=I+1
      IF ((DAT(I).GT.THRSMAX) .OR. (DAT(I).LT.THRSMIN)) THEN
         J=J+1
         INDX(J)=I
         L=0
         DO K=I,I+ENVLP
            L=L+1
            SUBARR(L)=DAT(K)
         END DO
         PP(J)=MAXVAL(SUBARR,MASK=SUBARR.NE.0.0)-
$              MINVAL(SUBARR,MASK=SUBARR.NE.0.0)
         IF (PP(J).LE.(1.05*(THRSMAX-THRSMIN))) THEN
            J=J-1
         END IF
            I=I+ENVLP
      END IF
   END DO

! Calculate sampling time and particle concentration
   STIM=N/(60.0*DAT(1))
   CONC=J/(FLOW*STIM)

! Compute average and standard deviation of PP array
   SUM=0.0
   DO I=1,J
      SUM=SUM+PP(I)
   END DO
   AVG=SUM/J

! Sort PP array (max to min)
   DO WHILE (UNSORTED)
      DONE='YES'
      DO I=1,(J-1)
         IF (PP(I).LT.PP(I+1)) THEN
            TEMP=PP(I)
            PP(I)=PP(I+1)
            PP(I+1)=TEMP
            TEMP=INDX(I)
            INDX(I)=INDX(I+1)
            INDX(I+1)=TEMP
            DONE='NO'
```

```
            END IF
         END DO
         IF (DONE.EQ.'YES') THEN
            UNSORTED=.FALSE.
         END IF
      END DO

   ! Open and write data to selected output file
      OPEN (11,FILE=FILEOUT)
      WRITE (11,'("Maximum threshold value:",F11.8)') THRSMAX
      WRITE (11,'("Minimum threshold value:",F11.8)') THRSMIN
      WRITE (11,'("Signal envelope:",I3," points")') ENVLP

      IF (J.EQ.0) THEN
         WRITE (11,'(/,/,"No particles detected!!!")')
      ELSE
         WRITE (11,'(/,I5," Particles detected")') J
         WRITE (11,'(/,"Flowrate: ",F6.2," L/min")') FLOW
         WRITE (11,'(/,"Concentration: ",F10.3," ppl")') CONC
         WRITE (11,'(/,"Average p-p voltage: ",F11.8," V")') AVG
         WRITE (11,'(/,"P-P values (V):",5X,"Signal start index:")')
         DO K=1,J
            WRITE (11,'(F11.8,18X,I10)') PP(K),INDX(K)
         END DO
      END IF
      CLOSE (11)
   END

************************* -- SUBROUTINES -- *************************

   SUBROUTINE THRSHOLD (THRSMIN,THRSMAX)
      PARAMETER (NMAX=1500000)
      CHARACTER FILENM*12
      REAL*8 THRSMIN,THRSMAX,T(NMAX),SUM,SUMSQ,AVG,STDEV,SD
      INTEGER N

   ! Ask for input file name
      WRITE (*,*) 'Enter file name (include file extension,',
     $            ' 12 characters maximum):'
      READ (*,*) FILENM

   ! Open and read the file selected by user
      OPEN (10,FILE=FILENM)
      N=0
      DO WHILE (.NOT. EOF (10))
         N=N+1
         READ (10,*) T(N)
      END DO
      CLOSE (10)

   ! Compute average and standard deviation of input data set
      SUM=0.0
      DO I=2,N
         SUM=SUM+T(I)
      END DO
      AVG=SUM/(N-1)

      SUMSQ=0.0
      DO I=2,N
```

```
      SUMSQ=SUMSQ+(T(I)-AVG)**2
    END DO
    STDEV=SQRT(SUMSQ/(N-2))

 ! The user can select how far away from the mean to set the
 ! thresholds
    WRITE (*,*) 'How many standard deviations away from the mean',
$               'do you want the thresholds to be set at?'
    READ (*,*) SD

    THRSMIN=AVG-(SD*STDEV)
    THRSMAX=AVG+(SD*STDEV)
    RETURN
 END
```

LIST OF REFERENCES

[1] Langer, G., An acoustic particle counter – preliminary results. *Journal of Colloid Science*, **20**, pp. 602-609, 1965.

[2] Langer, G., Status of acoustic particle counter research. *Powder Technology*, **2**, pp. 307-309, 1968/69.

[3] Karuhn, R. F., The development of a new acoustic particle counter for particle size analysis. *Proceedings of the First International Conference in Particle Technology, IIT Research Institute Chicago, IL*, pp. 202-207, 1973.

[4] Mills, T. E. and Chen, R.–H., Observations of an acoustic aerosol particle transducer. *Journal of Sound and Vibration*, **226(1)**, pp. 191-200, 1999.

[5] H.W.Liepmann and A.Roshko (1957) Elements of Gas Dynamics. New York:Wiley

[6] Chen, R.–H., Chaos, M., Haddad, G. F., and Mills, T. E., Effects of vortex shedding by particles in acoustical transducers. *Journal of Sound and Vibration*, **270**, pp. 473-479, 2004.

[7] TSI Incorporated, http://www.tsi.com/particle/products/partsize/3321.htm

[8] Auton, T. R., Hunt, J. C. R., M. Prud'homme, Journal of Fluid Mechanics 197 (1988): 24

[9] Stokes, G.G. "On the effect of the internal friction of fluids on the motion of pendulums." Transactions of the Cambridge Philosophical Society 9, Part II (1851): 8-106

[10] Oseen, C.W. "Über die Stokessche Formel und über die verwandte Aufgabe in der Hydrodynamik." Arkiv Mat., Astron. och Fysik 6, No. 29 (1910).

[11] Clift R., Grace J.R., and Weber M.E. Bubbles, Drops, and Particles. New York: Academic Press, 1978.

[12] White, F. M., Fluid Mechanics, 3rd ed., McGraw-Hill: New York, 1994.

[13] John, J. E. A. Gas Dynamics. 2nd ed. Englewood Cliffs: Prentice-Hall, 1984

[14] Akai, T. J. Applied Numerical Methods for Engineers. New York: John Wiley & Sons, 1994.

[15] Achenbach, E.," Vortex shedding from spheres," Journal of Fluid Mechanics 62 (1974): 209-221.

[16] Chen, R.–H. and Mills, T. E., Shape determination of aerosol particles using an acoustic transducer. Journal of Sound and Vibration, 232(3), pp. 652-658, 2000

[17] Duke Scientific Corporation, http://www.dukesci.com

[18] Mills, T. E. and Chen, R.–H., Aerosol particle concentration determined using an acoustic transducer. Journal of Sound and Vibration, 243(4), pp. 769-773, 2001.